Biomedicine & Pharmacotherapy 191 (2025) 118541

Contents lists available at ScienceDirect

Biomedicine & Pharmacotherapy

journal homepage: www.elsevier.com/locate/biopha

Insights into histone deacetylase inhibitors-induced cell death in cancer cell lines

María Fuentes-Baile [a], Pilar García-Morales [b], Elizabeth Pérez-Valenciano [a,b], Trinidad Mata-Balaguer [c], María P. Menéndez-Gutiérrez [d], Camino de Juan Romero [a,b], Álvaro Rodríguez-Lescure [e], Elena Martín-Orozco [f], Ricardo Mallavia [b], Víctor M. Barberá [a,g], Miguel Saceda [a,b,*]

[a] Unidad de Investigación, Fundación para el Fomento de la Investigación Sanitaria y Biomédica de la Comunidad Valenciana (FISABIO), Hospital General Universitario de Elche, Camí de l'Almazara, 11, Elche, Alicante 03203, Spain
[b] Instituto de Investigación, Desarrollo e Innovación en Biotecnología Sanitaria de Elche (IDiBE), Universidad Miguel Hernández, Avda. Universidad s/n, Ed. Torregaitán, Elche, Alicante 03202, Spain
[c] Departamento de Fisiología, Genética y Microbiología, Facultad de Ciencias, Universidad de Alicante, Alicante 03080, spain
[d] Centro Nacional de Investigaciones Cardiovasculares, Madrid, Spain
[e] Servicio de Oncología, Hospital General Universitario de Elche, FISABIO, Elche, Alicante 03203, Spain
[f] Department of Biochemistry and Molecular Biology B and Immunology, Murcia BioHealth Research Institute (IMIB), University of Murcia, Murcia, Spain
[g] Unidad de Genética Molecular, Hospital General Universitario de Elche, FISABIO, Camí de l'Almazara, 11, Elche, Alicante 03203, Spain

ARTICLE INFO

Keywords:
Histone deacetylase inhibitor
Cell-death mechanisms
Endoplasmic reticulum stress
Caspase-independent cell death
Serine protease inhibitor
Differential gene expression analysis

ABSTRACT

Histone deacetylase inhibitors (HDACis) induce cell death in many chemoresistant cancer models, suggesting their potential as alternative treatments for these malignancies. However, their efficacy in solid tumors remains limited. Therefore, understanding the molecular mechanisms underlying HDACi-induced cell death is essential for developing targeted activators of these pathways, enabling the selective elimination of chemoresistant cancer cells while minimizing the widespread transcriptional effects of HDACis. In this study, we investigated HDACi-induced cell death across models of different cellular origins to determine whether a universal molecular mechanism triggers this process. Our findings demonstrate that HDACi-induced cell death is TP53-independent, resistant to caspase inhibitors, and sensitive to serine protease inhibitors. This form of cell death requires intracellular calcium mobilization to induce mitochondrial depolarization. Using DNA arrays, apoptosis protein arrays, and ELISA assays, combined with siRNA-mediated gene silencing, we identified genes with a causal relationship to TSA-induced cell death. These include dual-specificity phosphatases such as DUSP3 and DUSP10; endoplasmic reticulum stress-related genes such as XBP1, MBTPS1, MBTPS2, and RPS6KA5; and other genes like BAX, AIF, EAF2, NANOS1, and CCNYL1. Our findings reveal novel potential targets for developing antineoplastic agents designed to exploit HDACi-induced cell death pathways, providing a strategy to overcome chemoresistance in cancer therapy.

1. Introduction

The acquisition of resistance to antineoplastic agents by tumor cells is a clinically relevant challenge associated with poor prognosis and the failure of cancer chemotherapy.

Chromatin structure regulation through histone modifications, such as acetylation and deacetylation, plays a crucial role in gene transcription [1]. In particular, histone hyperacetylation induced by histone deacetylase inhibitors (HDACis) can critically influence processes like apoptosis, cell proliferation, and differentiation [2].

* Corresponding author at: Unidad de Investigación, Fundación para el Fomento de la Investigación Sanitaria y Biomédica de la Comunidad Valenciana (FISABIO), Hospital General Universitario de Elche, Camí de l'Almazara, 11, Elche, Alicante 03203, Spain

E-mail addresses: maria.fuentes@fisabio.es (M. Fuentes-Baile), pgarcia@umh.es (P. García-Morales), elizabeth.perez@goumh.umh.es (E. Pérez-Valenciano), trinidad.mata@ua.es (T. Mata-Balaguer), mpmenendez@cnic.es (M.P. Menéndez-Gutiérrez), m.juan@umh.es (C. de Juan Romero), onkopinha@gmail.com, rodriguez_alvles@gva.es (Á. Rodríguez-Lescure), emartin@um.es (E. Martín-Orozco), r.mallavia@umh.es (R. Mallavia), barbera_vicjua@gva.es (V.M. Barberá), masceda@umh.es (M. Saceda).

https://doi.org/10.1016/j.biopha.2025.118541
Received 19 May 2025; Received in revised form 28 August 2025; Accepted 5 September 2025
Available online 12 September 2025

We and others have demonstrated that HDACis can induce cell death in several chemoresistant cancer models [3–6], suggesting their potential as an alternative treatment for chemoresistant cancers. Currently, several HDACis are being evaluated in clinical trials, both as monotherapies and in combination with other treatments [7]. To date, four HDACis have been approved by the Food and Drug Administration (FDA): vorinostat (SAHA) and romidepsin (FK228) for cutaneous T-cell lymphoma (CTCL), panobinostat (LBH589) for multiple myeloma, and belinostat (PXD-101) for peripheral T-cell lymphoma [8]. However, HDACis have shown limited efficacy in phase II clinical trials for most solid tumors [9–12]. Additionally, adverse effects ranging from mild (e.g., diarrhea, dehydration) to severe (e.g., cardiotoxicity, thrombocytopenia) have been reported in some patients [13].

The limited success of HDACi treatments in solid tumors may be attributed to their broad transcriptional effects. Differential gene expression studies reveal that HDACis impact thousands of genes, and the resulting epigenetic changes, combined with diverse cellular contexts, make treatment outcomes unpredictable. To overcome these limitations, second-generation inhibitors have been developed, including drugs targeting the bromodomain—an evolutionarily conserved 110-amino-acid domain within chromatin-associated proteins that interprets histone acetylation marks [14]. Furthermore, the use of nanoparticles as carriers for HDACis and other epigenetic drugs is being explored to enhance efficacy and reduce side effects [15].

Our experimental approach differs: rather than developing alternative HDACi formulations, we seek to determine whether a universal mechanism governs HDACi-induced cell death and whether this mechanism can be modulated independently of the broad transcriptional effects of HDACis. These strategy aims to minimize off-target effects and reduce adverse side effects.

Although the ability of HDACis to induce cell death is well stablished, the molecular mechanisms underlying this process remain unclear. While some studies suggest that HDACi-induced cell death involves caspase activation [2,16–19], our findings, supported by other research, indicate that this type of cell death can occur without caspase activation [6,20,21]. Whether caspase activation is essential for HDACi-induced cell death remains unresolved, and the role of p53 in this process also remains unclear.

This study aims to provide deeper insight into HDACi-induced cell death in chemoresistant cell lines. Given that discrepancies in previous findings may arise from the use of specific cell models, we investigated HDACi-induced cell death using Trichostatin A (TSA) across multiple cell models of different origins. Our objective was to determine whether a specific molecular mechanism underlies HDACi-induced cell death across various cell models. If such a mechanism exists, we aimed to identify its key features and assess whether cell death induction can be dissociated from the broad transcriptional effects of HDACis.

Our results demonstrate that HDACi-induced cell death is inhibited by serine protease inhibitors but not by caspase inhibitors across all tested cell models. This process is largely independent of p53 activation and requires AIF release, along with changes in the expression of Bcl-2 family members. Using differential gene expression analysis and siRNA-mediated gene silencing, we identified and validated several proteins involved in TSA-induced cell death across all tested models. Our findings indicate that intracellular calcium mobilization and endoplasmic reticulum stress are critical factors in TSA-induced cell death. Furthermore, we identified a set of genes associated with HDACi-induced cell death, establishing a causal relationship for many of these genes, including dual-specificity phosphatases, endoplasmic reticulum stress-related genes, and others.

Our study highlights novel potential targets for developing antineoplastic agents designed to combat chemoresistant tumors via the HDACi-induced cell death pathway.

2. Materials and methods

2.1. Cell lines and culture

L1210 and its daunomycin-resistant stable subline (L1210R) are murine leukemia cell lines. HL-60 and its resistant subline HL-60R are human promyelocytic leukemia cell lines. K562 and its resistant variant K562/Adr are human erythroleukemia cell lines. Al three cell lines are resistant to anthracyclines [22]. All hematopoietic cell lines were cultured as previously described [23].

Human pancreatic adenocarcinoma cell lines IMIM-PC-1, IMIM-PC-2, RWP-1, PANC-1, BxPC3, and Hs766T, as well as human urinary bladder carcinoma cell lines T-24, MGHU4, SW800, and VMCUB3, were kindly provided by Dr. Xavier Mayol (Instituto Municipal de Investigaciones Médicas, IMIM, Barcelona, Spain). Human colon carcinoma cell lines SW480, SW620, HT-29, and HGUE-C-1 were also used in this study. Breast carcinoma cell lines MCF-7 and its adriamycin-resistant subline MCF-7/Adr, as well as prostate carcinoma cell lines LNCap and PC3, were cultured as previously described [6].

Glioblastoma cell lines T-98, LN229, and glioblastoma primary culture-derived cell lines HGUE-GB-18 and HGUE-GB-42 were grown following previously established protocols [24].

2.2. Plasmids

The p53-EGFP chimera expression vector, pp53-EGFP (Clontech Laboratories Inc., CA, USA), contains a p53-EGFP expression cassette driven by the CMV immediate-early promoter. This vector also includes a neomycin resistance cassette controlled by the SV40 early promoter. Luciferase reporter plasmids under the control of endoplasmic reticulum stress elements (ERSE) were obtained from Qiagen (Hilden, Germany).

2.3. Transfection experiments

L1210, L1210R, RWP-1, IMIM-PC-2, and MCF-7 cells were transfected with plasmids expressing reporter proteins under the control of response elements for transcription factors of interest (e.g., TP53, endoplasmic reticulum stress-related factors), as previously described [24,25].

2.4. Determination of caspase activity

Caspase-3, −8, and −9 activities were measured using a colorimetric kit (Caspase-3, −8, and −9/Mch6 activity kits) according to the manufacturer's instructions. Recombinant caspases 3, 8, and 9 were assayed under the same conditions.

Caspase inhibition was performed by preincubating cells with specific inhibitors. The inhibitors used were:, Caspase-3 inhibitor I (DEVD-CHO, 25 μM), and a general caspase inhibitor (Z-VAD-FMK, 25 μM). Serine protease inhibitors included 4-(2-aminoethyl) benzenesulfonyl fluoride (AEBSF, 100 μM), Nα-Tosyl-Lys Chloromethyl Ketone (TLCK, 100 μM), and Nα-Tosyl-Phe Chloromethyl Ketone (TPCK, 1 μM). All inhibitors were added 30 min before 1 μM TSA treatment when applied in combination. All inhibitors mentioned in this section were purchased from Calbiochem (Darmstadt, Germany).

2.5. Flow cytometry analysis of cell cycle distribution

Cell lines were incubated with 1 μM TSA for up to 24 h. Cellular DNA content was analyzed using an Epics XL flow cytometer (Beckman Coulter Co., Miami, FL, USA) as previously described [5,6]. Non-viable cells were excluded based on abnormal size.

As required, cells were treated with HDACis in the presence or absence of cell-permeable caspase or serine protease inhibitors for up to 24 h before flow cytometry analysis. In the corresponding experiments, 1,2-Bis(2-aminophenoxy)ethane-N,N,N′,N′-tetraacetic acid tetrakis

(acetoxymethyl ester) (BAPTA-AM, 10 μM) and ethylene glycol-bis (β-aminoethyl ether)-N,N,N′,N′-tetraacetic acid (EGTA, 1 mM) were added 30 min before the addition of TSA.

2.6. Cell death determination

HDACi-induced cell death was assessed using various methods. The percentage of cells in the subG1 phase of the cell cycle was determined by flow cytometry. Additional confirmation was obtained by flow cytometry or fluorescence microscopy using an Annexin V-FITC commercial kit (Calbiochem, Darmstadt, Germany) or Hoechst 33342 (3 μg/mL) nuclear fragmentation staining.

Mitochondrial transmembrane potential disruption was evaluated using the Mitocapture™ Apoptosis Detection Kit (Calbiochem, Darmstadt, Germany) following the manufacturer's instructions.

2.7. Real-time RT-PCR

mRNA levels of AIF, Bax, Bcl-xL, DUSP10, XBP-1, MBTSP1, MBTSP2, EAF2, NANOS1, CCNYL1, and RPS6KA5 were quantified via real-time RT-PCR in untreated, TSA-treated, and siRNA-transfected cells, as previously described [24,26]. Briefly, total RNA was isolated using the NZY Total RNA Isolation Kit (NZYtech, Lisbon, Portugal), following the manufacturer's instructions. cDNA synthesis was performed using the High-Capacity cDNA Reverse Transcription Kit (Applied Biosystems™, Foster City, CA, USA) according to the manufacturer's protocol.

Quantitative PCR (qPCR) was conducted in 96-well plates using 10 μL NZYSpeedy qPCR Probe Master Mix (2x), ROX plus (NZYtech, Lisbon, Portugal), 1 μL predesigned TaqMan® Gene Expression Assays (Applied Biosystems, Foster City, CA, USA), and 4 μL cDNA, which was previously obtained. The Taqman Gene Expression Assays used were AIF (Hs00377585_m1), B*AX* (Hs00180269_m1), BCLXL (Hs00236329_m1), DUSP-10 (Hs00200527_m1), XBP1 (Hs00964359_m1), XBP1 spliced (Hs03929085_g1), MBTPS1 (Hs00921626_m1), MBTPS2 (Hs00210639_m1), EAF2 (Hs00218407_m1), NANOS1 (Hs00996068_s1), CCNYL1 (Hs00861771_g1), RPS6KA5 (Hs01046591_m1), and GAPDH (Hs02786624_g1) as endogenous control. All reactions were performed in triplicate, including non-template controls with water. Amplification was carried out using the QuanStudio®3 Real-Time PCR (Applied Biosystems, Foster City, CA, USA).

2.8. Immunocytochemistry

Cells were seeded in 24-well plates, treated as indicated, washed with 1x PBS, and fixed with methanol overnight at −20°C. Following PBS washing, cells were permeabilized for 5 min with 1x PBS containing 0.25 % Triton X-100 (Sigma). After washing with 1x PBS containing 0.5 % BSA (PBS-B, Sigma), blocking was performed with 1x PBS, 2 % BSA, and 0.5 % sodium azide for 30 min at room temperature.

Cells were then incubated overnight at 4°C with the primary antibody (mouse anti-AIF (E-1), sc-13116, Santa Cruz Biotechnology, Inc) diluted 1:100 in 0.5 % BSA, followed by three washes with PBS-B. Subsequently, cells were incubated for 30 min at room temperature and in the dark with goat anti-mouse IgG conjugated with fluorescein (Molecular Probes) diluted 1:30 and Hoechst stain at 3 μg/mL. Finally, cells were washed three times with PBS-B and analyzed by fluorescence microscopy.

2.9. siRNA-mediated inhibition of gene expression

IMIM-PC-2 cells were transfected using Lipofectamine™ RNAiMAX Transfection Reagent (Invitrogen, Carlsbad, CA, USA) with 20–25 nt target-specific siRNAs designed to knock down AIFM1 (AIF) and BAX gene expression. Specific siRNAs for AIFM1, BAX, and a negative control (sc-29193, sc-29212, and sc-37007, respectively) were purchased from Santa Cruz Biotechnology, Inc. (Santa Cruz, CA, USA) and assayed following the manufacturer's instructions.

Similarly, IMIM-PC-2, RWP-1 pancreatic carcinoma cell lines, and HGUE-GB-18 and HGUE-GB-42 glioblastoma primary culture-derived cell lines were transfected with siRNAs targeting DUSP10, XBP-1, MBTSP1, MBTSP2, EAF2, NANOS1, CCNYL1, and RPS6KA5 genes. These siRNAs, along with negative controls, were purchased from Invitrogen (Carlsbad, CA, USA) and used according to the manufacturer's protocol.

Specific gene knockdown was confirmed by real-time RT-PCR, as described in Section 2.7.

2.10. DNA array analysis

L1210, L1210R, RWP-1, PANC-1, IMIM-PC-1, IMIM-PC-2, Hs766T, and BxPC3 cells were treated with TSA (1 μM) in the presence or absence of AEBSF (100 μM) for 6 h. RNA was isolated using the NZY Total RNA Isolation Kit (NZYtech, Lisbon, Portugal) and analyzed using Affymetrix GeneChip® microarrays (PROGENIKA Biopharma S.A., Bizkaia, Spain).

cRNA synthesis followed the Affymetrix IVT Labeling Kit protocol, and purification was performed using the Affymetrix GeneChip Simple Cleanup Module. Hybridization and chip processing were performed according to the manufacturer's instructions. Software used included AGCC 1.1 and Expression Console™ (EC 1.1, Affymetrix®), with comparative analysis conducted using GeneChip® Operating Software (GCOS 1.4, Affymetrix®).

The microarrays employed were Mouse430_2.na21 for L1210 and L1210R cells, and HG-U133A_2.na22 and HG-U133_Plus_2.na26 for human pancreatic cell lines.

2.11. MAPK and AKT ELISA assays

RWP-1, IMIM-PC-2, and Hs766T pancreatic carcinoma cell lines were treated with TSA (1 μM) and AEBSF (100 μM) for 30 min to 24 h. Phosphorylation levels of MAPK pathway proteins (ERK 1/2, p38α, JNK 1/2/3) and AKT were assessed using InstantOne ELISA™ kits (eBioscience®, San Diego, CA, USA) following the manufacturer's instructions.

2.12. Proteasome activity assay

TSA-treated cells were harvested and incubated in a buffer containing 10 mM Tris (pH 7.5), 1 mM EDTA, and 20 % glycerol for 15 min on ice. Samples were centrifuged at 13,000 × g for 10 min at 4°C, and protein concentrations were determined. Protein extracts (10 μg) were then incubated in a reaction buffer with SDS and a fluorogenic substrate according to the manufacturer's instructions. Fluorescence was measured using a Fluostar Galaxy microplate fluorimeter (excitation: 370 nm, emission: 460 nm). Purified 20S proteasome served as a positive control, and Cells from the utilized cell lines were cultured in the presence of 10 μM of the proteasome inhibitors MG132 or PSI for 24 h and collected as mentioned above, and were used as a negative control to demonstrate that the use of the fluorogenic substrate employed to determine proteasome activity practically disappeared when this activity was blocked by the inhibitors.

2.13. Apoptosis-related protein array

Hs766T and BxPC3 pancreatic adenocarcinoma cell lines were treated with TSA (1 μM) in the presence or absence of AEBSF (100 μM) for 6–24 h. Cells were harvested and analyzed for apoptosis-related protein expression using the Proteome Profiler™ Array (R&D Systems, Inc., Minneapolis, MN, USA), according to the manufacturer's guidelines.

2.14. STRING database analysis

Protein interactions were analyzed using the STRING database (https://string-db.org/) [27].

2.15. Statistical analysis

Descriptive statistics were performed using GraphPad Prism v9. Mean and standard deviation values were calculated for gene expression, viability, and cell cycle data across all cell lines.

Normality was evaluated using the Shapiro-Wilk test, and homoscedasticity was assessed using Levene's test. Comparisons between two groups were conducted using the Student's *t*-test for parametric and homoscedastic datasets. The Mann-Whitney U-test was applied for non-parametric or heteroscedastic data. A p-value < 0.05 was considered statistically significant.

3. Results

3.1. p53 does not play a key role in HDACi-induced cell death

To assess whether p53 activation is an essential requirement for HDACi-induced cell death, as previously suggested [28–30], we used the L1210 and L1210R cell models. L1210 cells are resistant, whereas L1210R cells are sensitive to HDACi-induced cell death. First, we transiently transfected both cell lines with a reporter construct under the control of several p53 response elements. The results in Fig. 1 demonstrate that TSA treatment activates endogenous p53 in both cell lines. As a control, we transfected MCF-7 breast carcinoma cells, which are known to possess a wild-type p53 phenotype.

Finally, we compared the effect of TSA 1 μM on cell death induction across various cell lines from different tumor types with either mutated or wild-type TP53 (Table 1). The data indicate that a wild-type TP53 is not required for TSA-induced cell death. Furthermore, TSA successfully induced cell death in cell lines with null mutations, meaning complete loss of p53 expression.

3.2. HDACis-induced cell death is mostly a caspase-independent phenomenon

To determine whether caspase activation is required for HDACis-induced cell death, we analyzed whether cell death induction by HDACis correlates with an increase in caspases 3, 8, and 9 activities in all

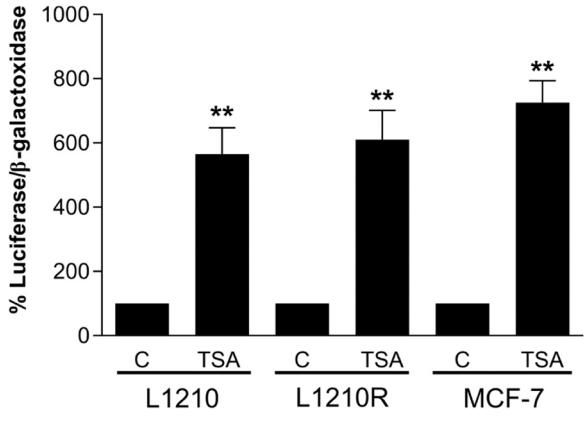

Fig. 1. TP53 protein activation levels. TP53 transcriptional activity was determined in L1210, L1210R, and MCF-7 cell lines in the presence and absence of TSA (1 μM) treatment by transient transfection assays with a TP53 reporter gene and a constitutively expressed β-galactosidase vector as an internal control for transfection efficiency. The mean percentage of TP53 activation normalized to β-galactosidase activity is shown. Error bars are SD ($n > 3$). ** Indicates a p-value < 0.01.

Table 1
Relationship between TP53 status and HDACi-induced cell death in cell lines of different origins. The table shows the cell line name, TP53 status (wild-type (Wt), mutated (Mut), unknown (Uk), or null), sensitivity to HDACi-induced cell death, and cancer type (murine leukemia (mL), human leukemia (hL), pancreatic carcinoma (PC), bladder carcinoma (BC), colon carcinoma (CC), breast carcinoma (BrC), prostate carcinoma (PrC) and glioblastoma (GB)).

Cell line	TP53 status	HDACi-induced cell death	Cancer type
L1210	Wt	Resistant	mL
L1210R	Wt	Sensitive	mL
HL−60	Null	Sensitive	hL
HL−60R	Null	Sensitive	hL
K−562	Null	Sensitive	hL
K562/Adr	Null	Sensitive	hL
IMIM-PC−1	Mut	Sensitive	PC
IMIM-PC−2	Mut	Sensitive	PC
RWP−1	Mut	Sensitive	PC
PANC−1	Mut	Sensitive	PC
BxPC3	Mut	Sensitive	PC
Hs766T	Wt	Resistant	PC
T−24	Mut	Sensitive	BC
MGHU4	Wt	Sensitive	BC
SW800	Wt	Sensitive	BC
VMCUB3	Mut	Sensitive	BC
HT−29	Mut	Sensitive	CC
SW620	Mut	Sensitive	CC
SW480	Mut	Sensitive	CC
HGUE-C−1	Wt	Sensitive	CC
MCF−7	Wt	Sensitive	BrC
MCF−7/Adr	Uk	Sensitive	BrC
LNCap	Null	Sensitive	PrC
PC3	Mut	Partially resistant	PrC
T−98	Mut	Sensitive	GB
LN229	Mut	Sensitive	GB
HGUE-GB−18	Mut	Sensitive	GB
HGUE-GB−42	Mut	Sensitive	GB

described cell lines. We also tested whether treatment with high concentrations of cell-permeable caspase inhibitors could partially or totally block HDACis-induced cell death. The results in Fig. 2 demonstrate that in most of the cell lines analyzed, HDACi treatment induces an increase in caspase activity, especially caspase 3. As an example, we show the data from L1210 and L1210R cells (Fig. 2A). Similar results (increase of caspase 3 activity) were found in HL-60, HL-60/Adr, K562 and K562/Adr cells (Fig. S1A). However, the different caspase inhibitors used alone or in combination do not block cell death induced by HDACis treatment in any of the tested cell lines (Fig. 2B). The concentrations of the different caspase inhibitors were selected because they effectively inhibited recombinant caspase 3 in vitro (Fig. S1B) as well as TSA-induced caspase-3 activation after 24 h of treatment in the L1210R cell line (Fig. S1C).

3.3. HDACis-induced cell death is a serine protease-dependent phenomenon

Given that increased caspase activity is, in many cases, dispensable for HDACis-induced cell death, we investigated which proteases assume the role of caspases when these were inhibited in our experiments. We found that the serine protease inhibitor AEBSF completely blocks the HDACis-induced cell death in all tested cell lines (Fig. 2C). Furthermore, other serine protease inhibitors, such as TLCK y TPCK, partially block TSA-induced cell death in several cell lines (Fig. 2D).

To confirm that serine protease inhibitors do not act as nonspecific caspase inhibitors, we tested these inhibitors *in vitro* against recombinant caspases, comparing their effects with specific inhibitors for those caspases (Fig. S1B). Next, we tested whether serine protease inhibitors are able to block HDACis-induced caspase activation *in vivo*. The results demonstrated that these inhibitors effectively block caspase 3 induction by TSA in the L1210R cell line (Fig. S1C).

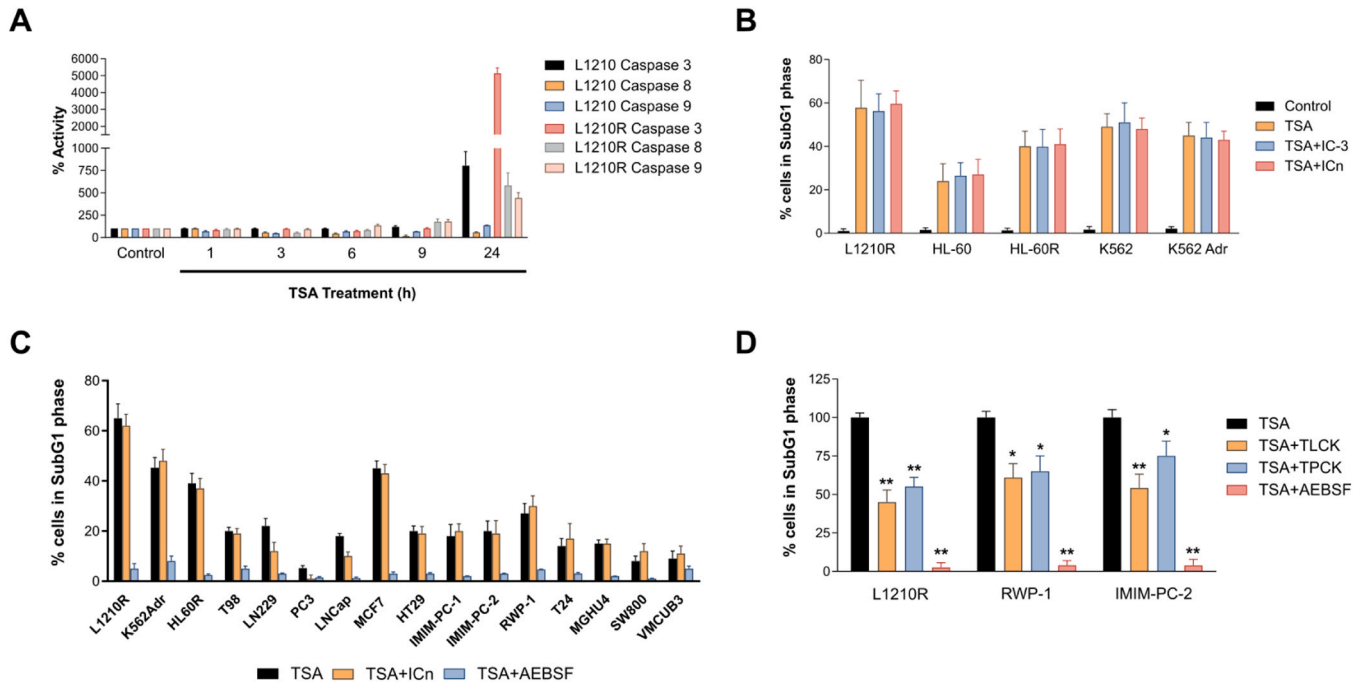

Fig. 2. Role of caspases and serin proteases in TSA-induced cell death. (A) Effect of TSA (1 μM) on caspases 3, 8 and 9 activities in L1210 and L1210R cell lines. Caspase activity was determined using specific colorimetric assays, and the percentage of activation relative to untreated cells is shown. (B) Percentage of cells in SubG1 phase in L1210R, HL-60, HL-60R, K562, and K562/Adr cell lines after treatment with TSA (1 μM) in the presence or absence of a caspase-3 inhibitor (25 μM) and a pan-caspase inhibitor (25 μM). (C) Percentage of cells in the SubG1 phase in a broad panel of cell lines after TSA (1 μM) treatment in the presence or absence of a pan-caspase inhibitor (25 μM) and a serin protease inhibitor (AEBSF, 100 μM). (D) Percentage of cells in the SubG1 phase of L1210R, RWP-1, and IMIM-PC-2 cell lines after TSA (1 μM) treatment in the presence or absence of serin protease inhibitors (TLCK 100 μM, TPCK 1 μM, and AEBSF 100 μM). DNA content distribution in the cell cycle was determined by flow cytometry after propidium iodide labeling, and the mean percentage of cells in the SubG1 phase is shown. Error bars represent SD ($n > 3$). * Indicates a p-value < 0.05 and ** p-value < 0.01.

3.4. HDACs-induced cell death requires the intracellular calcium mobilization and mitochondrial depolarization

To determine whether calcium is required for TSA-induced cell death, we preloaded cells with BAPTA-AM to prevent intracellular calcium mobilization before TSA treatment. TSA-induced cell death is almost abolished in BAPTA-AM-loaded cells (Fig. 3A), whereas EGTA, used to inhibit extracellular calcium uptake, does not affect TSA-induced cell death (Fig. S2). These results indicate that intracellular calcium mobilization is required for TSA-induced cell death. The requirement for intracellular calcium suggests a possible link to mitochondrial membrane depolarization. We tested this hypothesis in the L1210 /L1210R system, since L1210 is not induced to death by TSA, whereas L1210R is. We observed TSA-induced mitochondrial depolarization in L1210R but not in L1210 cells (Fig. 3B), and this depolarization was inhibited by pre-treatment with BAPTA-AM (10 μM) and, interestingly, also by the serine protease inhibitor AEBSF (100 μM) (Fig. S3).

3.5. HDACis-induced cell death requires AIF release and its nuclear localization

We had previously reported that AIF plays a role in HDACis-induced cell death in pancreatic adenocarcinoma cell lines [6]. To determine whether AIF also plays a role in cell lines of different origins, we examined AIF expression levels and nuclear localization, particularly in the L1210 and L1210R cell models (since in this system we have a

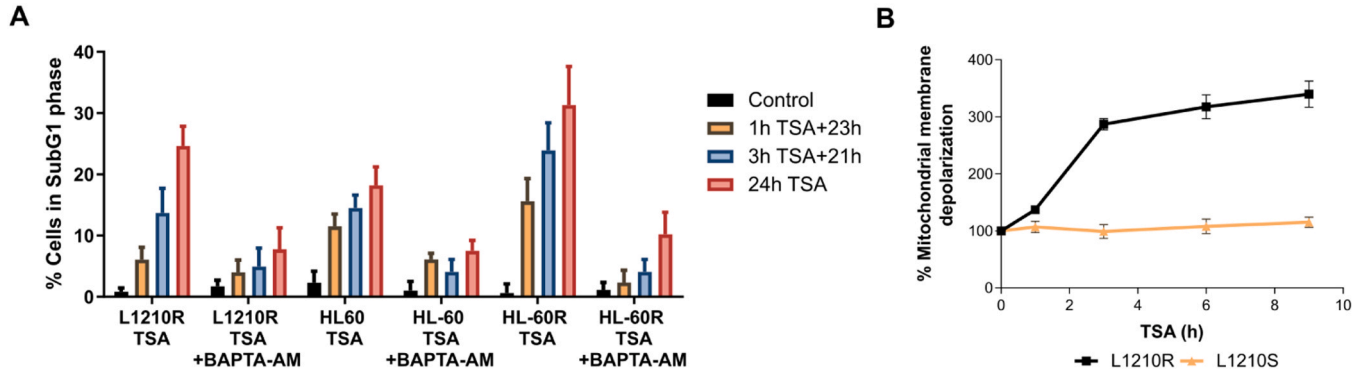

Fig. 3. Role of intracellular calcium mobilization and mitochondrial depolarization in TSA-induced cell death. (A) Percentage of cells in the SubG1 phase in L1210R, HL-60, and HL-60R cell lines after different treatment times (1, 3, and 24 h) with TSA (1 μM) in the presence or absence of BAPTA-AM (5 μM). DNA content distribution in the cell cycle was determined by flow cytometry after propidium iodide labeling, and the mean percentage of cells in the SubG1 phase is shown. (B) Mitochondrial membrane depolarization in L1210R and L1210 cell lines after 1, 3, 6, and 9 h of TSA (1 μM) treatment. Error bars represent SD ($n > 3$).

negative control which does not undergo cell death by TSA). As in pancreatic carcinoma, TSA treatment increases AIF levels in the L1210R cell line but not in the L1210 cell line (Fig. S4A). Nuclear localization of AIF after TSA treatment in L1210R was confirmed via immunostaining (Fig. S4B), as previously demonstrated in our publication on pancreatic carcinoma cell lines.

A similar increase in AIF protein levels and nuclear localization is observed after HDACis treatment in HL-60, HL-60R, K562 and K562/Adr cell lines (data not shown). Interestingly, the increase in AIF protein levels does not correlate with an increase in *AIF* mRNA, as determined by real time RT-PCR (Fig. S4A), suggesting that HDACis induce *AIF* expression via post-transcriptional regulation. The essential role of AIF in HDACi-induced cell death is further demonstrated by knocking down AIF gene expression using targeted siRNA in the pancreatic adenocarcinoma cell line IMIM-PC-2. Our results in Fig. 4A and B show that HDACis-induced cell death is reduced by AIF siRNA in parallel to decreased *AIF* gene expression, confirming AIF's critical role in this process.

3.6. Members of the Bcl-2 family are required for HDACis-induced cell death

Mitochondrial depolarization appears to be a requirement for HDACi-induced cell death, as a disruption in mitochondrial potential is observed in L1210R but not in L1210 cells (Fig. 3B). This suggests that changes in mitochondrial potential are associated with HDACi-induced cell death.

The involvement of Bcl-2 family members in HDACi-induced cell death was examined across different cell lines. We had published that TSA increases Bax levels without affecting Bcl-2 levels in pancreatic adenocarcinoma cell lines [6]. We observed changes in the expression of several Bcl-2 family members in all analyzed cell lines following TSA or SAHA treatment (Fig. S5). In pancreatic adenocarcinoma cell lines, there is an increase in a proapoptotic Bcl-2 family member, whereas in other cases, such as in L1210R cells, the main change is Bcl-2 downregulation, although Bax levels also increase.

Interestingly, the HDACi-induced increase in Bax protein levels in pancreatic [6] and colon carcinoma cell lines does not correlate with an increase in Bax mRNA levels, suggesting that HDACis regulate Bax expression at the post-transcriptional level (Fig. S6A). The post-transcriptional regulation of Bax and AIF may be linked to HDACi-induced inhibition of proteasome activity, which we have observed in these cell lines and will be discussed later in this section.

The crucial role of Bax in HDACi-induced cell death was confirmed through Bax knockdown using siRNA in IMIM-PC-2 pancreatic adenocarcinoma cells. As shown in Fig. 4C and D, HDACi-induced cell death is reduced following Bax silencing, in parallel with a decrease in Bax expression.

Another Bcl-2 family member differentially regulated by TSA in L1210 versus L1210R cells is Bcl-xL, which is downregulated by TSA in sensitive L1210R cells but remains unaffected in resistant L1210 cells (Fig. S6B). The downregulation of Bcl-xL by TSA has been observed in many other cell lines included in our study (Fig. S5).

Finally, we investigated whether Bid, a BH3-only member of the Bcl-2 family previously linked to HDACi-induced cell death, acts as a trigger for HDACi-mediated cell death. Regarding BID, transcriptomic analysis after 6 h of TSA treatment shows decreased expression in L1210R, IMIM-PC-1, and RWP-1 cells, while no changes or even slight increases are observed in the remaining cell lines, indicating no common pattern of BID mRNA expression. However, the key aspect of BID regulation lies in its proteolytic processing, whereby the full-length protein (22 kDa) is cleaved into its active truncated form, tBID (~15 kDa). Since BID is processed by caspases 8 and 10, and Fig. 2A shows that caspase-8 activation in L1210R (sensitive to TSA-induced cell death) occurs only after nearly 24 h of treatment, BID processing would represent a late event. Therefore, it cannot be considered as a trigger of TSA-induced cell death, in contrast to mitochondrial depolarization, which we have demonstrated to play a critical role in this process.

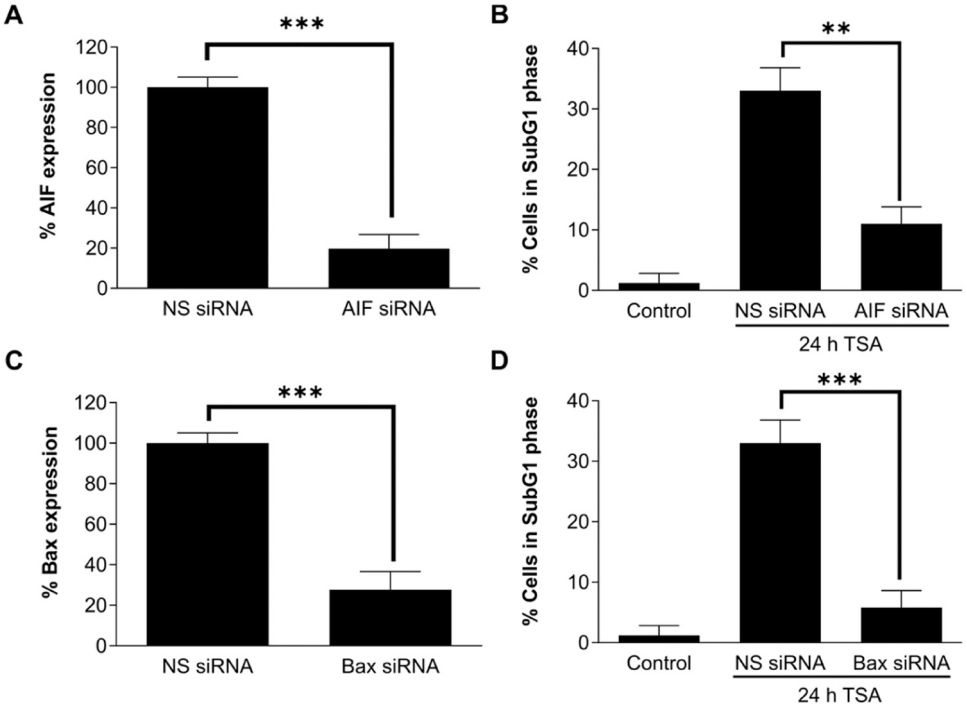

Fig. 4. Role of AIF and Bax in TSA-induced cell death. The IMIM-PC-2 cell line was transfected with a siRNA specific for AIF or Bax, or a non-specific siRNA as a control. (A, C) AIF and Bax mRNA levels were determined by RT-PCR. (B, D) Percentage of cells in the SubG1 phase of the IMIM-PC-2 cell line after treatment with TSA (1 μM) in the presence of a siRNA for AIF or Bax, or a non-specific siRNA as a control. DNA content distribution in the cell cycle was analyzed by flow cytometry after propidium iodide labeling, and the mean percentage of cells in the SubG1 phase is shown. Error bars represent SD ($n > 3$). ** Indicates a p-value < 0.01 and *** p-value < 0.001.

3.7. Differential gene expression studies highlight central role of dual phosphatases in HDACi-induced cell death

To identify specific genes involved in TSA-induced cell death, we employed a subtractive DNA array approach (Fig. 5). We selected genes whose expression increased or decreased after 6 h of treatment with 1 μM TSA in all TSA-induced cell death-sensitive cell lines. Data were obtained from DNA microarrays in L1210R, RWP-1, IMIM-PC-2, IMIM-PC-1, PANC1, and BxPC3. We excluded genes that were also regulated by TSA in the TSA-resistant cell lines L1210 and Hs766T. Further filtering was applied by selecting only genes whose TSA regulation was abolished in the presence of the serine protease inhibitor AEBSF, the only inhibitor capable to almost completely blocking TSA-induced cell death. This approach allowed us to identify fewer than 20 genes out of the more than 2500 regulated by TSA in each individual array.

Among the identified genes, we found two dual phosphatases, DUSP3 and DUSP10, whose expression levels in our gene expression array are shown in Table 2. DUSP3 is downregulated by TSA, and this effect was validated by RT-PCR in several pancreatic adenocarcinoma cell lines (Fig. 6A). Conversely, DUSP10 is upregulated by TSA, and this effect was validated by RT-PCR in the same cell lines used for DUSP3 expression studies (Fig. 6B). Furthermore, DUSP10 knockdown using a specific siRNA in pancreatic carcinoma and glioblastoma cell lines significantly decreased DUSP10 mRNA levels in all models tested (Fig. 6C). More importantly, this decrease in DUSP10 expression paralleled the reduction in TSA-induced cell death in the same cellular models (Fig. 6D), suggesting a cause relationship between TSA's effect on DUSP10 expression and its ability to induce cell death.

Given that DUSPs negatively regulate MAPK activity, we used specific ELISA assays to determine whether TSA differentially regulates MAPKs in TSA-sensitive versus TSA-resistant cells. Our results demonstrate that TSA 1 μM induces an increase in JNK kinase and P38 MAPK activity within the first 6 h of treatment (Fig. S7). An increase in ERK kinase activity was also observed after 24 h, a time frame too prolonged to implicate ERKs in TSA-induced cell death initiation. These effects on MAPKs activity were not observed in the TSA-resistant cell line Hs766T. Additionally, TSA treatment resulted in decreased AKT kinase activity.

3.8. HDACis-induced endoplasmic reticulum stress is required for TSA-induced cell death

Another interesting gene downregulated by TSA in our arrays is XBP1, which is typically associated with the cellular response to endoplasmic reticulum stress. After validating this downregulation by RT-PCR in pancreatic carcinoma cell lines (Fig. 7A), we investigated whether XBP1 was spliced by IRE-1 following TSA treatment, a key initial response to endoplasmic reticulum stress. We found that TSA induces XBP1 splicing activation in pancreatic carcinoma cells sensitive to TSA-induced cell death, but not in the Hs766T cell line, which is resistant to TSA-induced cell death (Fig. 7B). Since these data suggest that TSA induces endoplasmic reticulum stress, we first examined by RT-PCR whether GRP78 (HSPA5) expression, the initial sensor of endoplasmic reticulum stress, was affected by TSA treatment. As shown in Fig. 7C, TSA significantly increases HSPA5 mRNA levels in TSA-sensitive pancreatic carcinoma cell lines.

Furthermore, we transfected two TSA-sensitive pancreatic carcinoma cell lines with a reporter gene under the control of several endoplasmic reticulum stress-response elements (ERSE). Our results indicate that TSA induces transcription mediated by the ERSE (Fig. 7D), suggesting an increase in endoplasmic reticulum stress. Given the known relationship between endoplasmic reticulum stress and proteasome activity, we next assessed whether TSA treatment affected proteasome activity in sensitive cell lines. Our results show that TSA inhibits proteasome activity in IMM-PC-2 and RWP-1 cell lines (Fig. 7E). Finally, to determine whether TSA-induced cell death is directly linked to XBP1, we knocked down XBP1 expression using a specific siRNA in pancreatic carcinoma and glioblastoma cell lines. Our results demonstrate that when XBP1 expression is knocked down (Fig. 7F), TSA-induced cell death is significantly inhibited (Fig. 7G).

To further investigate the relationship between TSA-induced cell death and endoplasmic reticulum stress, we examined the expression of proteins related to this type of cellular stress. Fig. 8A presents a

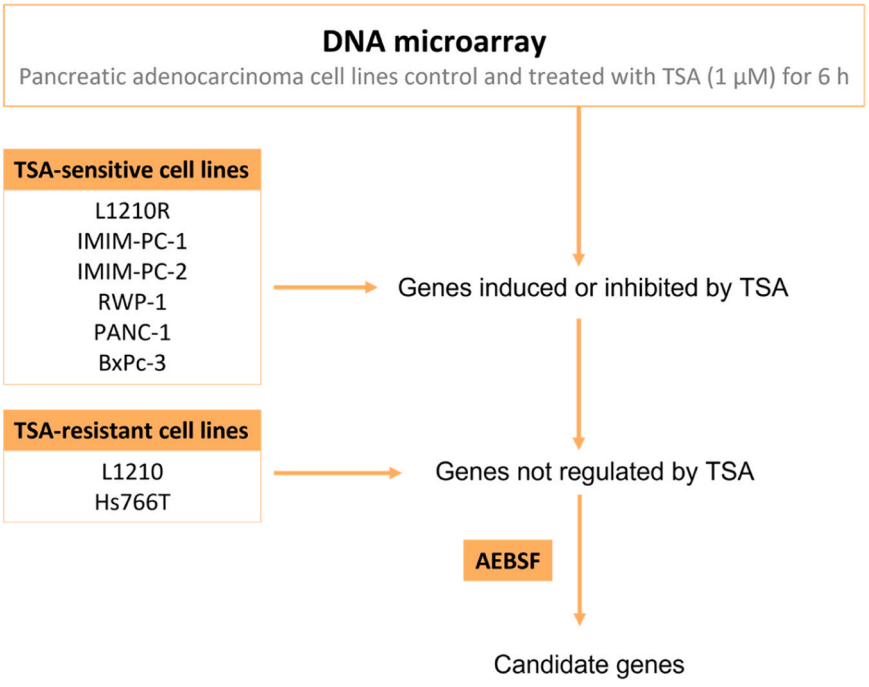

Fig. 5. Schematic representation of DNA arrays performed on different cell lines after 6 h of TSA (1 μM) treatment. The arrays were conducted in TSA-sensitive and TSA-resistant cell lines, with or without AEBSF treatment. Genes regulated by TSA in the sensitive cell lines but not in the resistant ones were selected, as well as genes that lost their response to TSA after AEBSF (100 μM) treatment.

Table 2
Expression levels of DUSP3 and DUSP10 genes obtained from DNA arrays in TSA-sensitive cell lines (L1210R, IMIM-PC-1, IMIM-PC-2, RWP-1, and PANC-1) and TSA-resistant cell lines (L1210 and Hs766T). The percentage of expression in TSA-treated cells is shown relative to untreated cells.

%Expression/ untreated cells	TSA-sensitive cell lines					TSA-resistant cell lines	
	L1210R	IMIM-PC-1	IMIM-PC-2	RWP-1	PANC-1	L1210	Hs766T
DUSP3	57 ± 4.6	56 ± 5.6	37 ± 2.9	40 ± 5.3	61 ± 6.2	87 ± 5.1	92 ± 6.1
DUSP10	373 ± 12	141 ± 3.6	179 ± 7.5	246 ± 8.7	221 ± 8.5	100 ± 3.4	99 ± 4.7

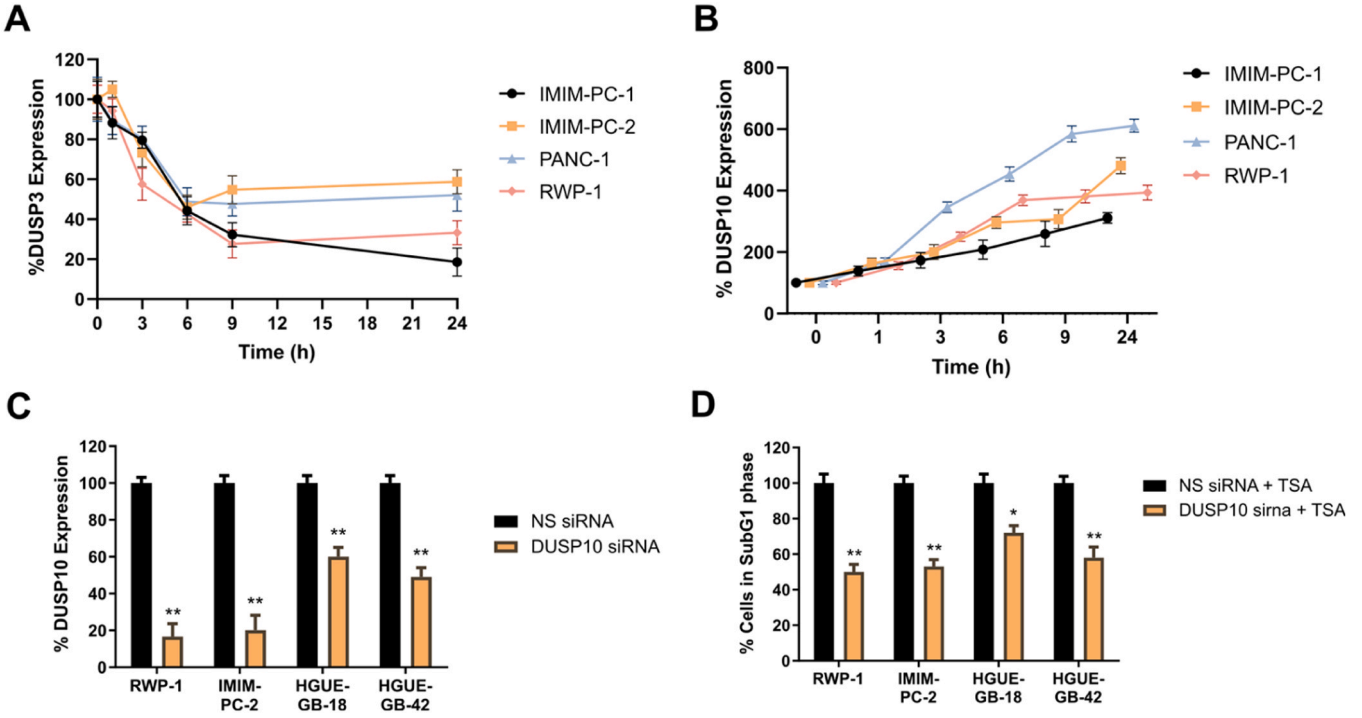

Fig. 6. Role of DUSP3 and DUSP10 in TSA-induced cell death. DUSP3 (A) and DUSP10 (B) mRNA levels were obtained by RT-PCR after treating IMIM-PC-1, IMIM-PC-2, RWP-1, and PANC-1 cell lines for 1, 3, 6, 9, and 24 h with TSA (1 μM). DUSP10 expression (C) and the percentage of cells in the SubG1 phase (D) in RWP-1, IMIM-PC-2, HGUE-GB-18, and HGUE-GB-42 cell lines after treatment with TSA (1 μM) in the presence of a siRNA for DUSP10 or a non-specific siRNA (NS) used as a control. The mRNA levels were determined by RT-PCR, and the percentage of expression relative to cells transfected with NS siRNA is shown. The distribution of DNA content in the cell cycle was determined by flow cytometry after propidium iodide labeling, and the mean percentage of cells in the SubG1 phase is shown. Error bars represent SD ($n < 3$). * Indicates a p-value < 0.05 and ** p-value < 0.01.

schematic representation of key proteins modified during endoplasmic reticulum stress, while Fig. 8B shows the effect of TSA treatment in one TSA-sensitive cell line. Notably, TSA regulates several stress-response proteins, with some being downregulated, such as Nrf2 (NFE2L2), while others, such as IRE1, are upregulated. To confirm the role of endoplasmic reticulum stress in TSA-induced cell death, we analyzed data from our DNA arrays.

Three genes or gene families were consistently induced in TSA-sensitive cell lines following TSA treatment. One of these is RPS6KA5, a kinase linked to different stress conditions. Additionally, members of the ATF6 transcription factor family, particularly CREB3L2, were identified in pancreatic carcinoma cell lines. Lastly, KDELR3, an endoplasmic reticulum protein involved in the unfolded protein response (UPR), was also found. Based on the roles of these proteins, we knocked down RPS6KA5 and the sequential proteases SP1 (MBTSP1) and SP2 (MBTSP2), required for ATF6 activation in the Golgi apparatus. Figs. 8C and 9 show that knockdown was successfully achieved in pancreatic adenocarcinoma and glioblastoma cell lines, leading to a significant reduction in TSA-induced cell death in both models.

We also identified three additional genes in our DNA arrays whose knockdown with specific siRNAs resulted in a decrease in TSA-induced cell death. These genes are EAF2, NANOS1, and CCNYL1 (Fig. 9A, B).

3.9. Apoptotic protein profiling and other techniques identify additional proteins related to HDACi-induced cell death

Our findings regarding AIF and BAX suggest that TSA does not regulate these genes at the transcriptional level but rather through post-transcriptional mechanisms. To identify other cell death-related proteins that might be activated by TSA but were not detected in our DNA arrays due to post-transcriptional regulation, we conducted a cell death-related protein array. This analysis was performed in a TSA-sensitive cell line (BxPC3) in the presence or absence of AEBSF, and in a TSA-resistant cell line (Hs766T). We focused on proteins that were either upregulated or downregulated by TSA in BxPC3 but not in Hs766T. To refine our selection further, we included only those proteins whose TSA-dependent regulation was abolished after AEBSF (100 μM) treatment. Based on these criteria, we identified DR5, HIF, HSP27, and PON2 (Fig. S8).

3.10. Protein interaction analysis shows that proteins related to endoplasmic reticulum stress and WNT signaling pathways may play important roles in HDACis-induced cell death

Thus far, we have found that TSA-induced cell death is significantly inhibited by specific siRNAs targeting AIF (AIFM1), BAX, CCNYL1,

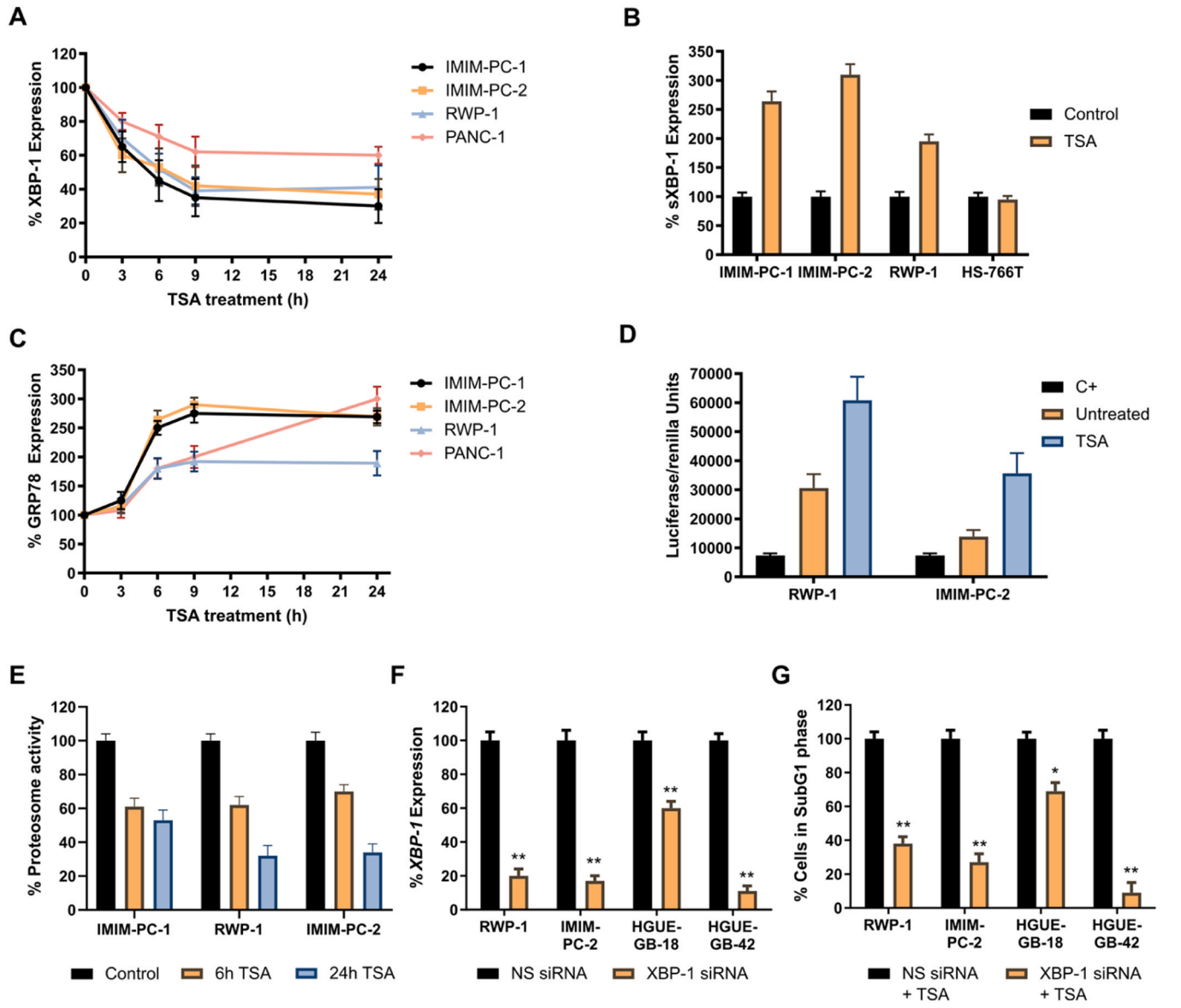

Fig. 7. Role of endoplasmic reticulum stress in TSA-induced cell death. XBP-1 (A) and GRP78 (C) mRNA levels were obtained by RT-PCR after treating IMIM-PC-1, IMIM-PC-2, RWP-1, and PANC-1 cell lines for 1, 3, 6, 9, and 24 h with TSA (1 μM). (B) XBP-1 spliced mRNA levels were obtained by RT-PCR after treating IMIM-PC-1, IMIM-PC-2, RWP-1, and Hs766T cell lines with TSA (1 μM). The percentage of expression in TSA-treated cells is plotted relative to untreated cells. (D) RWP-1 and IMIM-PC-2 cell lines were transfected with a luciferase expression plasmid under the control of endoplasmic reticulum stress response elements (ERSE). The plasmid also contains a renilla expression unit under a constitutively active promoter as an internal control for transfection efficiency. Transfected cells were treated with 1 μM TSA for 24 h, and luciferase and renilla expression were determined using a luminometer. The graph shows the ratio of luciferase to renilla expression under each condition. (E) IMIM-PC-1, RWP-1, and IMIM-PC-2 cell lines were treated with or without 1 μM TSA for 6 and 24 h, and proteasome activity was determined. DUSP10 expression (F) and the percentage of cells in the SubG1 phase (G) in RWP-1, IMIM-PC-2, HGUE-GB-18, and HGUE-GB-42 cell lines after treatment with TSA (1 μM) in the presence of a siRNA for XBP-1 or a non-specific siRNA (NS) used as a control. The mRNA levels were determined by RT-PCR, and the percentage of expression relative to cells transfected with NS siRNA is shown. The distribution of DNA content in the cell cycle was determined by flow cytometry after propidium iodide labeling, and the mean percentage of cells in the SubG1 phase is shown. Error bars represent SD ($n < 3$). * Indicates a p-value < 0.05 and ** p-value < 0.01.

EAF2, NANOS1, RPS6KA5, MBTPS1, MBTPS2, XBP-1, and DUSP10. Additionally, we identified other proteins regulated by TSA in sensitive but not in resistant cell lines. The genes encoding these proteins include BCL2L1, DUSP3, HSPA5, ZSG, ARL13B, BLR2, TIAGLN3, ELMO2, FCHSD1, HBP1, MGAT4A, TXNIP, TTBK2, PI12, RNF24, and CSNK2A2, along with proteins identified through the cell death protein array (DR5, HIF, HSP27, and PON2). Finally, AKT, P38, and JNK (1,2,3) have been shown to be regulated by TSA in TSA-sensitive cell lines.

In some cases, we have insights into how these genes are functionally linked to TSA-induced cell death. For instance, MGAT4A is involved in Golgi apparatus transport, HSPA5 serves as a key sensor of endoplasmic reticulum stress, and TXNIP is also implicated in this type of stress. To explore potential interactions among these proteins, we used the STRING database (Fig. 10A). Additionally, to establish a hierarchy among the genes involved in TSA-induced cell death, we analyzed whether silencing a specific gene with siRNA affected the expression of the other nine genes that we knocked down (Fig. 10B).

The analysis of the protein interaction network (Fig. 10A) reveals several key observations. First, it is evident that the P38 and JNK kinases play a crucial role in the life-death balance of TSA-treated cells, as their phosphorylation increases following TSA treatment (Fig. S7). Additionally, well-known inhibitors of these kinases, such as DUSP10, have been shown to be causally linked to TSA-induced cell death in different cell models (Fig. 6). Second, the endoplasmic reticulum stress clearly

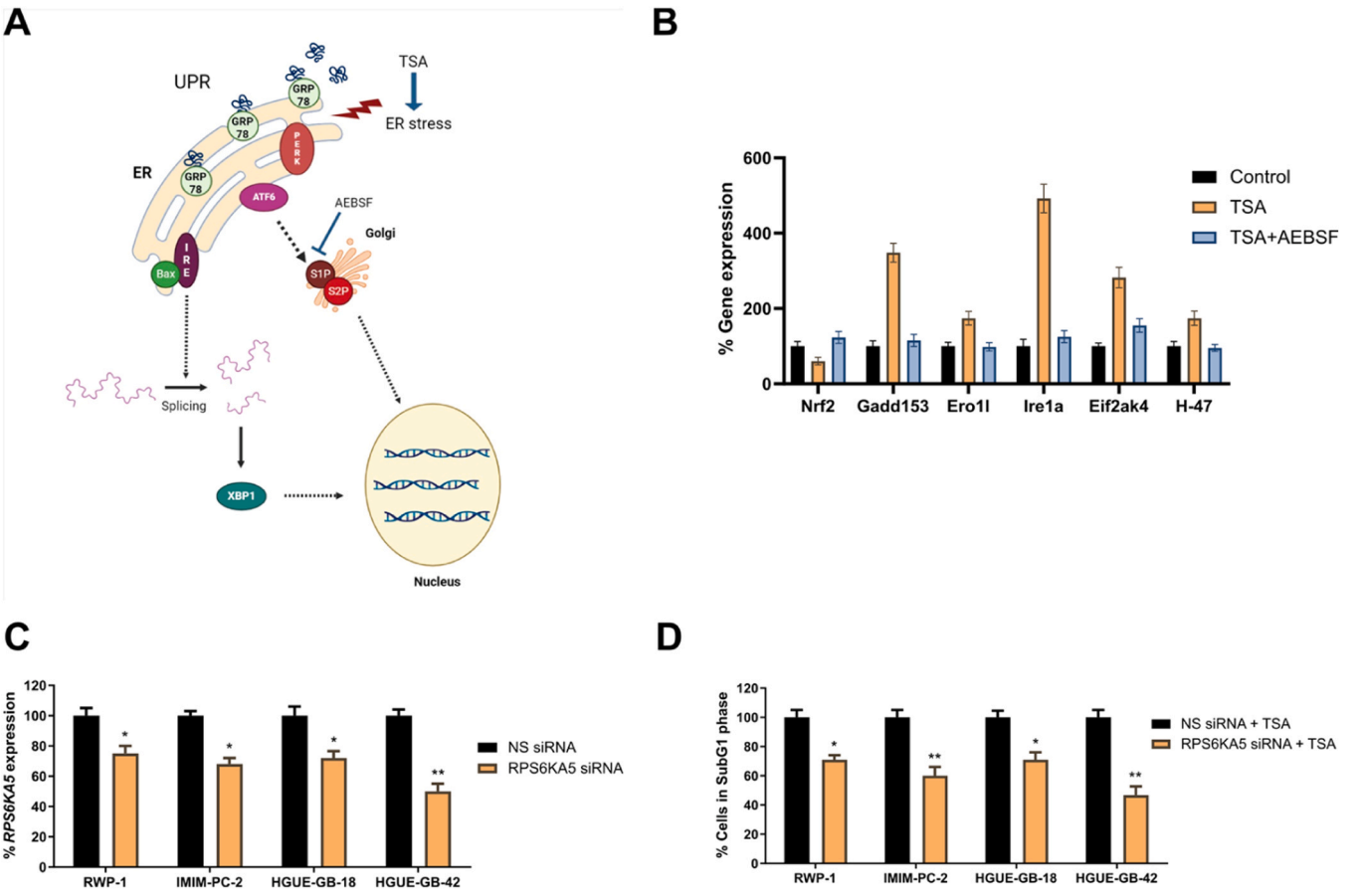

Fig. 8. Effect of TSA on the expression of endoplasmic reticulum stress-related proteins. (A) Schematic of key proteins modified after endoplasmic reticulum stress. (B) mRNA levels of Nrf2, Gadd153, Ero1l, Ire1a, Eif2ak4, and H-47 were obtained by RT-PCR after treating or not treating the L1210R cell line with TSA (1 μM) for 1 h, and with TSA in combination with AEBSF (100 μM). The percentage of expression in TSA-treated cells is plotted relative to untreated cells. RPS6KA5 expression (C) and the percentage of cells in the SubG1 phase (D) in RWP-1, IMIM-PC-2, HGUE-GB-18, and HGUE-GB-42 cell lines after treatment with TSA (1 μM) in the presence of a siRNA for RPS6KA5 or a non-specific siRNA (NS) used as a control. The mRNA levels were determined by RT-PCR and the percentage of expression relative to cells transfected with NS siRNA is shown. The distribution of DNA content in the cell cycle was determined by flow cytometry after propidium iodide labeling, and the mean percentage of cells in the SubG1 phase is shown. Error bars represent SD ($n < 3$). * Indicates a p-value < 0.05 and ** p-value < 0.01.

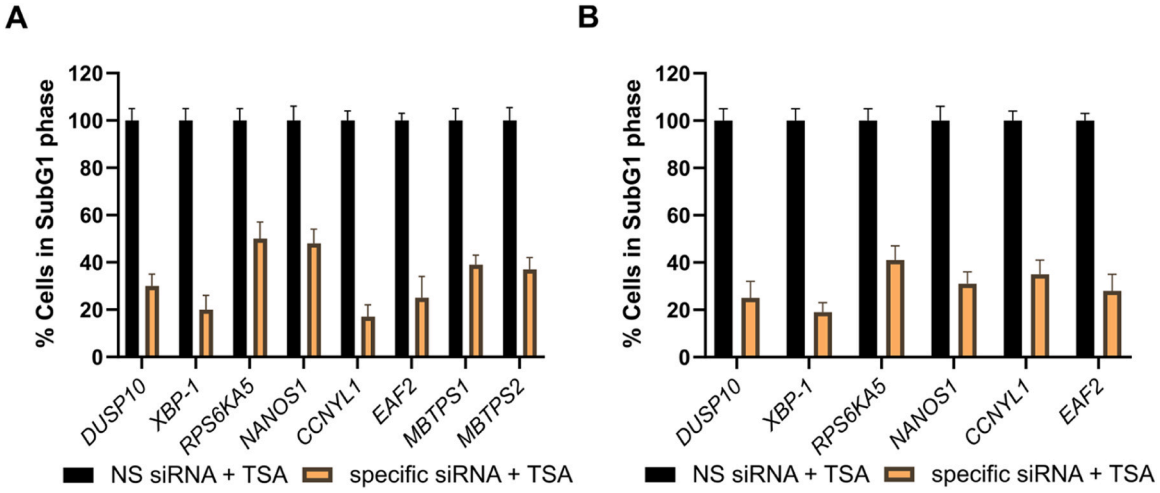

Fig. 9. Genes involved in TSA-induced cell death. Percentage of cells in the SubG1 phase in RWP-1 (A) and IMIM-PC-2 (B) cell lines after TSA treatment (1 μM) in the presence of a specific siRNA or a non-specific (NS) siRNA used as a control. DNA content distribution in the cell cycle was determined by flow cytometry after propidium iodide labeling. The mean percentage of cells in the SubG1 phase is shown. Error bars represent SD ($n < 3$).

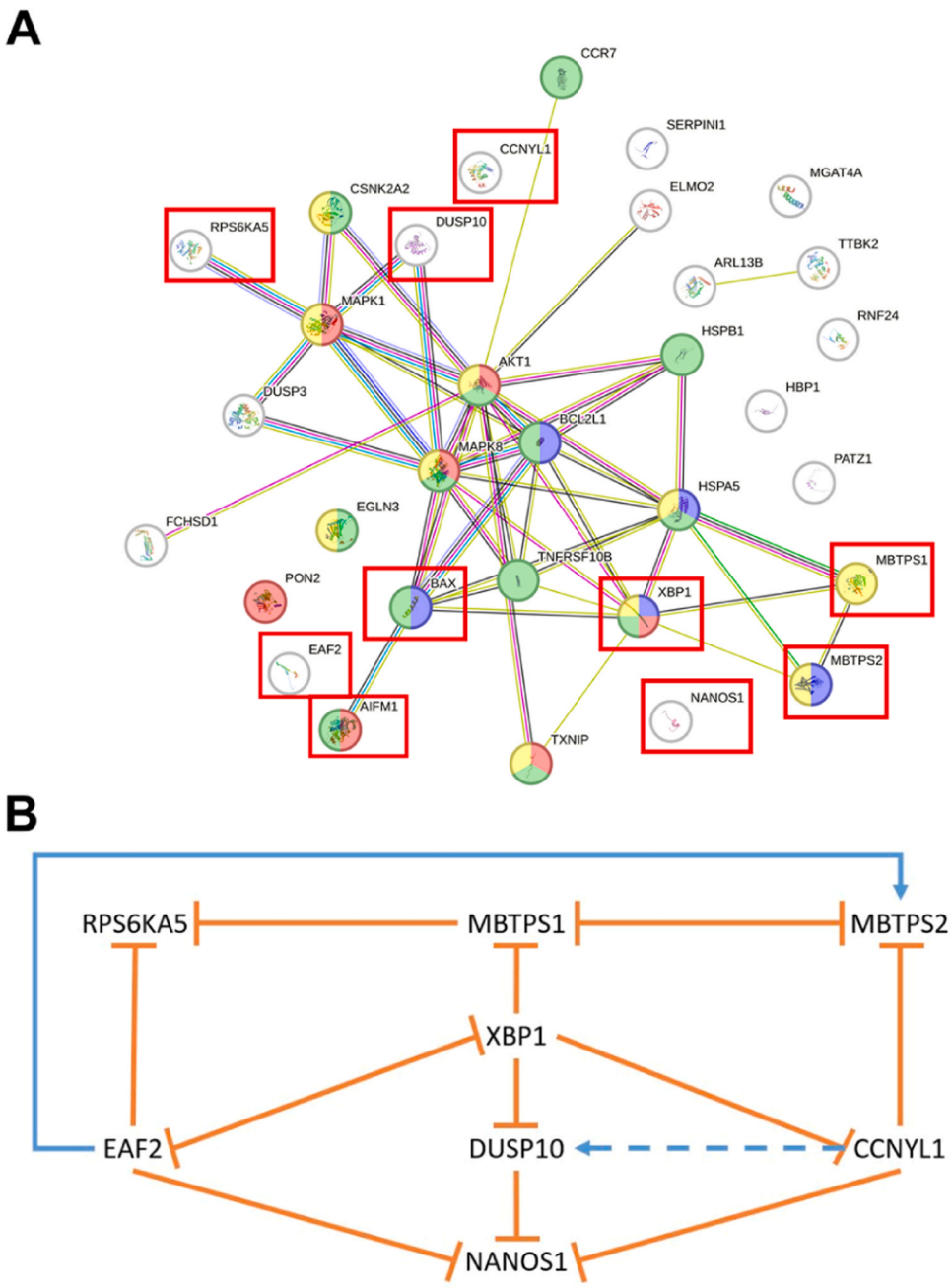

Fig. 10. Relationship between TSA-regulated genes. (A) Network representation of interactions between TSA-regulated proteins, obtained using the STRING database. Genes marked in blue are involved in endoplasmic reticulum stress response, those in red participate in the oxidative stress response, those in green regulate cell death processes, and those in yellow are involved in stress responses. Red boxes indicate genes directly associated with TSA-induced cell death (B) Schematic representation of the interactions among TSA-regulated genes, determined by RT-PCR after siRNA-mediated knockdown. Blue lines indicate increased expression, orange lines represent a decreased expression, and dashed lines indicate a moderate increase in expression.

triggers TSA-induced cell death in the same models, with a strong relationship between endoplasmic reticulum stress and MAPK pathways also being apparent (Fig. 10A). Third, and perhaps one of the most intriguing findings, is that three genes -EAF2, NANOS1, and CCNYL1- which have been shown to have a cause-effect relationship with TSA-induced cell death, appear to have no interaction with each other or with other genes identified in our STRING database search. These genes have recently been linked to a WNT signaling pathway that regulates not only transcriptional processes but also critical post-transcriptional processes in the cell [31–35], as will be discussed in the appropriate section.

In Fig. 10B, the analysis of reciprocal regulation among TSA-induced cell death genes highlights XBP-1 as a central regulator, directly or indirectly controlling the expression of all other key genes (Fig. 10A). This further underscores the role of endoplasmic reticulum stress as a key driver of TSA-induced cell death. Additionally, we observed a cross-regulation between EAF2, NANOS1, and CCNYL1, which are linked to WNT signaling, and other TSA-regulated genes. Interestingly, EAF2 appears to have a regulatory function similar to that of XBP-1, and a direct cross-regulatory relationships between EAF2 and XBP-1 suggest an interplay between WNT signaling and endoplasmic reticulum stress, a connection that will be discussed in the corresponding section.

4. Discussion

To identify alternative cell death pathways that remain active after the acquisition of chemoresistance, we tested many potential inducers of cell death in several cancer cell lines exhibiting the multidrug resistance (MDR) phenotype, as well as in intrinsically resistant cell lines of different origins. Given that HDACis are being investigated as novel antineoplastic agents [17,36,37], we analyzed their effects on our chemoresistant cell lines.

Our findings [5,6], in agreement with previous studies [38–40], demonstrate that HDACis effectively induce cell death in many cancer cell lines with the MDR phenotype, as well as in some intrinsically resistant cell lines. Notably, HDACi-induced cell death occurs at lower concentrations in chemoresistant cells compared to non-transformed cells [41], highlighting their potential clinical relevance. However, the efficacy of HDACis in solid tumors has been disappointing, likely due to drug instability, toxicity, and, most critically, off-target effects due to their broad impact on transcription [42,43]. To address this limitations, different strategies are being explored. One approach involves developing more selective HDACis targeting specific HDACs or bromodomain-containing proteins, which recognize acetylated marks on histones and other proteins [14]. Another strategy employs nanoparticles to enhance the targeted delivery of HDACis or other epigenetic drugs, thereby increasing drug concentration at tumor sites, improving stability, and reducing side effects [15].

Our research follows a distinct approach, focusing on two key questions: first, whether there exists a universal molecular mechanism that triggers HDACi-induced cell death, and second, if such a mechanism exists, whether it can be activated without inducing the broad transcriptional effects associated with HDACis. Despite numerous studies, the mechanisms underlying HDACi-induced cell death in chemoresistant cells remain unclear, and some puzzling questions arise from the different reports.

Some studies have suggested that p53 plays a crucial role in HDACi-induced cell death [44,45]. However, our results challenge this assumption. First, in the murine leukemia cell line L1210 (resistant to TSA-induced cell death) and its derived cell line L1210R (sensitive to TSA), p53 was activated by TSA, as demonstrated by transient transfection with a p53 reporter construct (Fig. 1). Second, TSA and SAHA induced cell death in p53-null HL-60 and HL-60R cells (Table 1). Third, TSA treatment triggered cell death in HT-29, SW620, IMIM-PC-1, IMIM-PC-2 and RWP-1 cell lines, all of which harbor different p53 mutations (Table 1). Although one study suggested that HDACis might act via activation of specific p53 mutations [46], our data do not support a pivotal role of p53 in HDACis-induced cell death.

Our results indicate that HDACis-induced cell death is not a caspase-dependent process. First, in IMIM-PC-1, IMIM-PC-2, and RWP-1 pancreatic carcinoma cell lines, HDACis did not significantly increase caspase activation, and both general and caspase-specific inhibitors failed to prevent cell death [6]. Second, although HDACis led to caspase activation (primarily caspase 3) in L1210R (Fig. 2A), HL-60, HL-60R, K-562, K562/Adr (Fig. S1A), and HT-29 cells, and also in other cell lines, caspase inhibitors, alone or in combination, could not block HDACi-induced cell death, at high concentrations (Fig. 2B, C). Third, caspase activation via the mitochondrial pathway requires cytochrome c release, which occurs later than other hallmarks of cell death, such as mitochondrial depolarization, annexin staining, etc. Time-course experiments further confirmed that caspase-3 activation and cytochrome c release are late events in L1210R cells (data not shown). Thus, caspase activation is unlikely to be primary trigger of HDACi-induced cell death.

Conversely, our findings reveal a crucial role for serine proteases in HDACi-induced cell death. In all tested cell lines, AEBSF, a serine protease inhibitor, completely blocked HDACis-induced cell death (Fig. 2C). Additional inhibitors, TLCK and TPCK, also significantly reduced cell death (Fig. 2D), implicating serine proteases in this process. Specifically, ucf-101, an inhibitor of the Omi/ HtrA2 serine protease, blocked HDACi-induced cell death in several pancreatic adenocarcinoma cell lines [6], suggesting that Omi/HtrA2 is involved. However, since ucf-101 itself induces cell death in hematopoietic cell lines, we cannot conclude that Omi/HtrA2 is the sole serine protease mediating HDACi-induced cell death across all cell models, just in pancreatic adenocarcinoma and multiple myeloma cell lines [6,47].

Another key finding is that the observed caspase activation in many cell lines is a late consequence of serine protease activation. Supporting this, AEBSF and other serine protease inhibitors failed to inhibit recombinant caspase activity (Fig. S1B), indicating that their effects are specific. Furthermore, these inhibitors completely abrogated HDACi-induced caspase activation in cell extracts, suggesting that caspase activation is a downstream effect of serine protease activity in early-stage HDACi-induced cell death (Fig. S1C). This mechanism may explain why HDACis induce cell death in Pgp-expressing cell lines despite the protective effects of Pgp against caspase-dependent apoptosis [48].

In agreement with our previous reports in pancreatic adenocarcinoma and multiple myeloma cell lines [6,47], we found that HDACis induce the release and nuclear translocation of AIF in other cell lines (Fig. S4B). Knockdown of AIF via siRNA significantly reduced HDACi-induced cell death in pancreatic carcinoma cells (Fig. 4A, B), underscoring its role in this pathway.

The Bcl-2 family also plays a crucial role in HDACis-induced cell death [6,49–51]. In pancreatic adenocarcinoma cells, HDACis increase the levels of Bax, a pro-apoptotic Bcl-2 family member [6] (Fig. S6A). Similar Bax upregulation was observed in HL-60, HL-60R, and other cell lines (data not shown). Notably, Bax knockdown via siRNA inhibited HDACi-induced cell death in pancreatic carcinoma cells (Fig. 4C, D). Interestingly, in L1210R cells, HDACis not only increased Bax levels but also reduced Bcl-2 expression. These findings suggest that HDACi-induced cell death depends on shifting the balance between pro- and anti-apoptotic Bcl-2 family members in favor of cell death. The importance of the Bax/Bcl-2 switch in achieving apoptosis in chemoresistant cells has been highlighted by other authors [52,53].

Another Bcl-2 family member that appears to be regulated in many of the cell models studied is Bcl-xL, whose expression is downregulated (Fig. S6B). However, this downregulation does not occur in the TSA-resistant cell lines L1210 and Hs766T, suggesting that Bcl-xL may play a role in TSA-induced cell death.

A controversial aspect is the role of different BH-3-only members of the Bcl-2 family in HDACi-induced cell death. While it is well established that many of these proteins are activated after HDACi treatment in various cell models [19,54–56], the key question remains whether their activation is a cause or consequence of HDACi-induced cell death. Our findings suggest that, at least in the case of Bid, its cleavage does not act as a trigger for HDACi-induced cell death, despite previous reports suggesting a more prominent role [57]. This conclusion is based on the time course of cell death induction and Bid cleavage.

An interesting hypothesis is that the key trigger for HDACi-induced cell death may be the alteration of the Bcl-2/Bax ratio via increased Bax expression, rather than a competition between Bax and a BH-3-only protein. In this regard, the effects of TSA on proteasome activity in pancreatic adenocarcinoma cell lines (Fig. 7E), which have also been observed in colon carcinoma cell lines [58], may explain the increase in AIF and Bax protein levels without a corresponding increase in their mRNAs (Fig. S4A). This could account for reports on HDACi-induced post-transcriptional regulation of p27 and NF-kB [59] and the collaborative effect of HDACis and proteasome inhibitors [60].

We have demonstrated that HDACi-induced cell death depends on mitochondrial depolarization (Fig. 3B), which may be triggered by intracellular calcium mobilization (Fig. 3A). Interestingly, mitochondrial depolarization is inhibited both by the calcium chelator BAPTA-AM and by the serine protease inhibitor AEBSF, which is able to block TSA-induced cell death in all tested models (Fig. S3), as well as by the disruption of the balance between Bcl-2 family members. Taken

together, our results suggest that this process results in Bax-mediated mitochondrial depolarization, leading to the release of AIF and Omi/HtrA2, and, in some cases, a delayed release of cytochrome c and subsequent caspase activation [6]. Increasing evidence supports a relationship between the Bcl-2 family and the regulation of intracellular calcium mobilization from the endoplasmic reticulum [61–63]. Thus, it is likely that TSA and other HDACis induce calcium release from the endoplasmic reticulum by modulating the balance between pro- and anti-apoptotic Bcl-2 family members.

The significance of the endoplasmic reticulum–mitochondria axis in HDACi-induced cell death is reinforced by multiple lines of evidence. Our differential gene expression analysis between TSA-sensitive and TSA-resistant cell lines, including both murine and human models, as well as hematopoietic and solid tumor cell lines, identified a small set of genes whose regulation by TSA disappears in cells treated with the serine protease inhibitor AEBSF (Fig. 5). Notably, among the TSA-regulated genes, XBP-1 was identified (Fig. 7B), underscoring the involvement of the endoplasmic reticulum stress pathway. Our siRNA experiments (Fig. 7F, G) demonstrated a causal relationship between XBP-1 expression and TSA-induced cell death. Furthermore, additional endoplasmic reticulum stress-related proteins, such as GPR78, IRE1, NRF2, and RPS6KA5, were also regulated by TSA (Figs. 7C, 8). This was further supported by transient transfection experiments using a reporter gene under ERSE regulation (Fig. 7D) and confirmation of TSA-induced proteasome inhibition (Fig. 7E), which has also been reported by other authors [64]. In this sense, recent articles have pointed out the relationship between ER stress and AIF release, particularly in TP53 wild-type cell lines. The differential expression of AIF in different cell lines could be linked to varied responses to HDACi treatment and may underlie potential resistance mechanisms [65]. However, as we have shown in this study, HDACi can exert beneficial effects even in cell lines that are resistant to therapy and in those deficient in p53.

Regardless of the precise mechanisms, our findings establish that HDACi-induced cell death is a caspase-independent, a serine protease-dependent process, requiring either increased expression of pro-apoptotic Bcl-2 family members or decreased expression of their anti-apoptotic counterparts.

Finally, our results demonstrate a causal relationship between HDACi-mediated regulation of EA2F, NANOS1, and CCNYL1 and the induction of cell death in both cell models (Fig. 9) and primary cultures from diverse origins (data not shown). Notably, EAF2, NANOS1, and CCNYL1 have been linked to both canonical and non-canonical WNT signaling pathways [31–35]. Increasing evidence supports a connection between WNT signaling and various effects of HDACis in the same cell models [66,67], including proliferation control, cell survival, drug resistance, stem cell maintenance, and immune evasion [68–73]. Our findings suggest that modifying WNT signaling could mimic HDACi-induced cell death while avoiding the broad transcriptional effects associated with HDACi treatment.

An intriguing possibility is that a single, universal mechanism triggered by HDACis may lead to distinct forms of cell death depending on the cellular context. In addition to the numerous studies linking HDACi-induced cell death to classical apoptosis and autophagy, emerging evidence now implicates these agents in ferroptosis and necroptosis [74–78]. This is not unexpected, as previous reports have associated HDACis with the generation of reactive oxygen species (ROS) and their regulation via the transcription factor Nrf2 [79,80], as well as with alterations in iron metabolism [81].

Notably, a growing body of literature connects ferroptosis with the WNT signaling [82–84]. This association is particularly relevant in light of our findings, which indicate that three WNT-related genes significantly influence TSA-induced cell death across different cellular models. These observations raise the possibility that HDACi-induced cell death, particularly in glioblastoma models, may involve ferroptosis—a hypothesis that warrants further investigation.

Funding

This study has been funded by Instituto de Salud Carlos III and co-funded by the European Union (FEDER) through the projects PI08/0901, PI12/02025 and PI22/00824 M.S and M.S and C.d.J.R (PI22/00824), Consellería de Innovación, Universidades, Ciencia y Sociedad Digital from Generalitat Valenciana (CIAICO/2022/081) given to M.S. This study was also funded by FISABIO intramural grant through the projects UGP-20–135 granted to M.S.

CRediT authorship contribution statement

María Fuentes-Baile: Writing – original draft, Visualization, Validation, Software, Methodology, Investigation, Data curation. **Miguel Saceda:** Writing – review & editing, Writing – original draft, Supervision, Resources, Methodology, Funding acquisition, Formal analysis, Conceptualization. **Víctor M. Barberá:** Validation, Investigation, Data curation. **Ricardo Mallavia:** Writing – review & editing, Formal analysis. **Elena Martin-Orozco:** Formal analysis. **Álvaro Rodríguez-Lescure:** Writing – review & editing, Resources, Funding acquisition. **Camino de Juan Romero:** Writing – review & editing, Resources, Funding acquisition, Formal analysis. **Maria P. Menendez-Gutierrez:** Validation, Investigation. **Trinidad Mata Balaguer:** Validation, Methodology, Investigation. **Elizabeth Pérez-Valenciano:** Visualization, Validation, Investigation. **Pilar García-Morales:** Validation, Methodology, Investigation.

Declaration of Competing Interest

The authors declare no conflict of interest.

Acknowledgments

The authors thank IMIM for generously providing us with many of the cell lines used in this work.

Appendix A. Supporting information

Supplementary data associated with this article can be found in the online version at doi:10.1016/j.biopha.2025.118541.

Data availability

The microarray data have been deposited at the Gene Expression Omnibus (GEO) database under accession number GSE30287

References

[1] W.K. Kelly, P.A. Marks, Drug insight: histone deacetylase inhibitors - development of the new targeted anticancer agent suberoylanilide hydroxamic acid, Nat. Clin. Pr. Oncol. 2 (3) (2005) 150–157, https://doi.org/10.1038/NCPONC0106.

[2] J. Zhang, Q. Zhong, Histone deacetylase inhibitors and cell death, Cell Mol. Life Sci. 71 (20) (2014) 3885–3901, https://doi.org/10.1007/S00018-014-1656-6.

[3] Q. Xu, X. Liu, S. Zhu, X. Hu, H. Niu, X. Zhang, et al., Hyper-acetylation contributes to the sensitivity of chemo-resistant prostate cancer cells to histone deacetylase inhibitor trichostatin a, J. Cell Mol. Med 22 (3) (2018) 1909–1922, https://doi.org/10.1111/JCMM.13475.

[4] E.S. José-Enériz, N. Gimenez-Camino, X. Agirre, F. Prosper, HDAC inhibitors in acute myeloid leukemia, Cancers (Basel) 11 (11) (2019) 1794, https://doi.org/10.3390/CANCERS11111794.

[5] M.D. Castro-Galache, J.A. Ferragut, V.M. Barbera, E. Martín-Orozco, J. M. Gonzalez-Ros, P. Garcia-Morales, et al., Susceptibility of multidrug resistance tumor cells to apoptosis induction by histone deacetylase inhibitors, Int J. Cancer 104 (5) (2003) 579–586, https://doi.org/10.1002/IJC.10998.

[6] P. García-Morales, A. Gómez-Martínez, A. Carrato, I. Martínez-Lacaci, V. M. Barberá, J.L. Soto, et al., Histone deacetylase inhibitors induced caspase-independent apoptosis in human pancreatic adenocarcinoma cell lines, Mol. Cancer Ther. 4 (8) (2005) 1222–1230, https://doi.org/10.1158/1535-7163.MCT-04-0186.

[7] R. Jenke, N. Reßing, F.K. Hansen, A. Aigner, T. Büch, Anticancer therapy with HDAC inhibitors: mechanism-based combination strategies and future perspectives, Cancers (Basel) 13 (4) (2021) 634, https://doi.org/10.3390/cancers.
[8] R. Hai, D. Yang, F. Zheng, W. Wang, X. Han, A.M. Bode, et al., The emerging roles of HDACs and their therapeutic implications in cancer, Eur. J. Pharm. 931 (2022) 175216, https://doi.org/10.1016/j.ejphar.2022.175216.
[9] S.C. Modesitt, M. Sill, J.S. Hoffman, D.P. Bender, A phase II study of vorinostat in the treatment of persistent or recurrent epithelial ovarian or primary peritoneal carcinoma: a gynecologic oncology group study, Gynecol. Oncol. 109 (2) (2008) 182–186, https://doi.org/10.1016/J.YGYNO.2008.01.009.
[10] J. Vansteenkiste, E. Van Cutsem, H. Dumez, C. Chen, J.L. Ricker, S.S. Randolph, et al., Early phase II trial of oral vorinostat in relapsed or refractory breast, colorectal, or non-small cell lung cancer, Invest N. Drugs 26 (5) (2008) 483–488, https://doi.org/10.1007/S10637-008-9131-6.
[11] H.J. Mackay, H. Hirte, T. Colgan, A. Covens, K. MacAlpine, P. Grenci, et al., Phase II trial of the histone deacetylase inhibitor belinostat in women with platinum resistant epithelial ovarian cancer and micropapillary (LMP) ovarian tumours, Eur. J. Cancer 46 (9) (2010) 1573–1579, https://doi.org/10.1016/J.EJCA.2010.02.047.
[12] L.R. Molife, G. Attard, P.C. Fong, V. Karavasilis, A.H.M. Reid, S. Patterson, et al., Phase II, two-stage, single-arm trial of the histone deacetylase inhibitor (HDACi) romidepsin in metastatic castration-resistant prostate cancer (CRPC), Ann. Oncol. 21 (1) (2010) 109–113, https://doi.org/10.1093/ANNONC/MDP270.
[13] J.J. McClure, X. Li, C.J. Chou, Advances and challenges of HDAC inhibitors in cancer therapeutics, Adv. Cancer Res 138 (2018) 183–211, https://doi.org/10.1016/BS.ACR.2018.02.006.
[14] M. Shao, L. He, L. Zheng, L. Huang, Y. Zhou, T. Wang, et al., Structure-based design, synthesis and in vitro antiproliferative effects studies of novel dual BRD4/HDAC inhibitors, Bioorg. Med. Chem. Lett. 27 (17) (2017) 4051–4055, https://doi.org/10.1016/J.BMCL.2017.07.054.
[15] M. Dasko, B. De Pascual-Teresa, I. Ortín, A. Ramos, HDAC inhibitors: innovative strategies for their design and applications, Molecules 27 (3) (2022) 715, https://doi.org/10.3390/molecules27030715.
[16] J.E. Bolden, W. Shi, K. Jankowski, C.Y. Kan, L. Cluse, B.P. Martin, et al., HDAC inhibitors induce tumor-cell-selective pro-apoptotic transcriptional responses, Cell Death Dis. 4 (2) (2013) e519, https://doi.org/10.1038/cddis.2013.9.
[17] T. Eckschlager, J. Plch, M. Stiborova, J. Hrabeta, Histone deacetylase inhibitors as anticancer drugs, Int J. Mol. Sci. 18 (7) (2017) 1414, https://doi.org/10.3390/IJMS18071414.
[18] P. Gong, Y. Wang, Y. Jing, Apoptosis induction by histone deacetylase inhibitors in cancer cells: role of Ku70, Int. J. Mol. Sci. 20 (7) (2019) 1601, https://doi.org/10.3390/IJMS20071601.
[19] M. Sanaei, F. Kavoosi, Effect of zebularine in comparison to trichostatin a on the intrinsic and extrinsic apoptotic pathway, cell viability, and apoptosis in hepatocellular carcinoma SK-Hep 1, human colorectal cancer SW620, and human pancreatic cancer PaCa-44 cell lines, Iran. J. Pharm. Res. 20 (3) (2021) 310–323, https://doi.org/10.22037/IJPR.2021.115097.15196.
[20] U. Natarajan, T. Venkatesan, V. Radhakrishnan, S. Samuel, A. Rathinavelu, Differential mechanisms of cell death induced by HDAC inhibitor SAHA and MDM2 inhibitor RG7388 in MCF-7 cells, Cells 8 (1) (2018) 8, https://doi.org/10.3390/CELLS8010008.
[21] A. Hrzenjak, M.L. Kremser, B. Strohmeier, F. Moinfar, K. Zatloukal, H. Denk, SAHA induces caspase-independent, autophagic cell death of endometrial stromal sarcoma cells by influencing the mTOR pathway, J. Pathol. 216 (4) (2008) 495–504, https://doi.org/10.1002/PATH.2434.
[22] M.V. Camarasa, M.D. Castro-Galache, E. Carrasco-García, P. Garcia-Morales, M. Saceda, J.A. Ferragut, Differentiation and drug resistance relationships in leukemia cells, J. Cell Biochem. 94 (1) (2005) 98–108, https://doi.org/10.1002/JCB.20278.
[23] F. Soto, R. Planells-Cases, J.M. Canaves, A.V. Ferrer-Montiel, J. Aleu, F. Gamarro, et al., Possible coexistence of two independent mechanisms contributing to anthracycline resistance in leukaemia P388 cells, Eur. J. Cancer 29A (15) (1993) 2144–2150, https://doi.org/10.1016/0959-8049(93)90050-P.
[24] M.P. Ventero, M. Fuentes-Baile, C. Quereda, E. Perez-Valenciano, C. Alenda, P. Garcia-Morales, et al., Radiotherapy resistance acquisition in glioblastoma. Role of SOCS1 and SOCS3, PLoS One 14 (2) (2019) e0212581, https://doi.org/10.1371/JOURNAL.PONE.0212581.
[25] S.V. Angeloni, M.B. Martin, P. Garcia-Morales, M.D. Castro-Galache, J.A. Ferragut, M. Saceda, Regulation of estrogen receptor-alpha expression by the tumor suppressor gene p53 in MCF-7 cells, J. Endocrinol. 180 (3) (2004) 497–504, https://doi.org/10.1677/JOE.0.1800497.
[26] M. Fuentes-Baile, P. García-morales, E. Pérez-Valenciano, M.P. Ventero, J.M. Sanz, C. de Juan Romero, et al., Cell death mechanisms induced by CLytA-DAAO chimeric enzyme in human tumor cell lines, Int J. Mol. Sci. 21 (22) (2020) 8522, https://doi.org/10.3390/ijms21228522.
[27] D. Szklarczyk, A.L. Gable, D. Lyon, A. Junge, S. Wyder, J. Huerta-Cepas, et al., STRING v11: protein–protein association networks with increased coverage, supporting functional discovery in genome-wide experimental datasets, Nucleic Acids Res. 47 (D1) (2019) D607–D613, https://doi.org/10.1093/NAR/GKY1131.
[28] J.A. Vrana, R.H. Decker, C.R. Johnson, Z. Wang, W.D. Jarvis, V.M. Richon, et al., Induction of apoptosis in U937 human leukemia cells by suberoylanilide hydroxamic acid (SAHA) proceeds through pathways that are regulated by Bcl-2/Bcl-XL, c-Jun, and p21CIP1, but independent of p53, Oncogene 18 (50) (1999) 7016–7025, https://doi.org/10.1038/sj.onc.1203176.
[29] L.F. Fröhlich, M. Mrakovcic, C. Smole, K. Zatloukal, Molecular mechanism leading to SAHA-induced autophagy in tumor cells: evidence for a p53-dependent pathway, Cancer Cell Int. 16 (1) (2016) 68, https://doi.org/10.1186/S12935-016-0343-0.
[30] M. Mrakovcic, J. Kleinheinz, L.F. Fröhlich, p53 at the crossroads between different types of HDAC Inhibitor-Mediated cancer cell death, Int. J. Mol. Sci. 20 (10) (2019) 2415, https://doi.org/10.3390/IJMS20102415.
[31] X. Wan, W. Ji, X. Mei, J. Zhou, J.X. Liu, C. Fang, et al., Negative feedback regulation of Wnt4 signaling by EAF1 and EAF2/U19, PLoS One 5 (2) (2010) e9118, https://doi.org/10.1371/JOURNAL.PONE.0009118.
[32] X. Ma, J.X. Liu, Eafs control erythroid cell fate by regulating c-myb expression through wnt signaling, PLoS One 8 (5) (2013) e64576, https://doi.org/10.1371/JOURNAL.PONE.0064576.
[33] K. Feng, H.K. Guo, Eaf2 protects human lens epithelial cells against oxidative stress-induced apoptosis by wnt signaling, Mol. Med. Rep. 17 (2) (2018) 2795–2802, https://doi.org/10.3892/MMR.2017.8246.
[34] N. Oulhen, S.Z. Swartz, L. Wang, A. Wikramanayake, G.M. Wessel, Distinct transcriptional regulation of Nanos2 in the germ line and soma by the wnt and delta/notch pathways, Dev. Biol. 452 (1) (2019) 34–42, https://doi.org/10.1016/J.YDBIO.2019.04.010.
[35] L. Zeng, C. Cai, S. Li, W. Wang, Y. Li, J. Chen, et al., Essential roles of cyclin Y-Like 1 and cyclin y in dividing Wnt-Responsive mammary Stem/Progenitor cells, PLoS Genet. 12 (5) (2016) e1006055, https://doi.org/10.1371/JOURNAL.PGEN.1006055.
[36] A.K.A. Bass, M.S. El-Zoghbi, E.S.M. Nageeb, M.F.A. Mohamed, M. Badr, G.E.D. A. Abuo-Rahma, Comprehensive review for anticancer hybridized multitargeting HDAC inhibitors, Eur. J. Med. Chem. 209 (2021) 112904, https://doi.org/10.1016/J.EJMECH.2020.112904.
[37] F. Dang, W. Wei, Targeting the acetylation signaling pathway in cancer therapy, Semin Cancer Biol. 85 (2022) 209–218, https://doi.org/10.1016/J.SEMCANCER.2021.03.001.
[38] H. Kim, S.N. Kim, Y.S. Park, N.H. Kim, J.W. Han, H.Y. Lee, et al., HDAC inhibitors downregulate MRP2 expression in multidrug resistant cancer cells: implication for chemosensitization, Int. J. Oncol. 38 (3) (2011) 807–812, https://doi.org/10.3892/IJO.2010.879.
[39] Q. Xu, X. Liu, S. Zhu, X. Hu, H. Niu, X. Zhang, et al., Hyper-acetylation contributes to the sensitivity of chemo-resistant prostate cancer cells to histone deacetylase inhibitor trichostatin a, J. Cell Mol. Med. 22 (3) (2018) 1909–1922, https://doi.org/10.1111/JCMM.13475.
[40] K. Kerl, D. Ries, R. Unland, C. Borchert, N. Moreno, M. Hasselblatt, et al., The histone deacetylase inhibitor SAHA acts in synergism with fenretinide and doxorubicin to control growth of rhabdoid tumor cells, BMC Cancer 13 (2013) 286, https://doi.org/10.1186/1471-2407-13-286.
[41] P. Papeleu, T. Vanhaecke, G. Elaut, M. Vinken, T. Henkens, S. Snykers, et al., Differential effects of histone deacetylase inhibitors in tumor and normal Cells—What is the toxicological relevance? Crit. Rev. Toxicol. 35 (4) (2005) 363–378, https://doi.org/10.1080/10408440590935639.
[42] T. Chiba, O. Yokosuka, M. Arai, M. Tada, K. Fukai, F. Imazeki, et al., Identification of genes up-regulated by histone deacetylase inhibition with cDNA microarray and exploration of epigenetic alterations on hepatoma cells, J. Hepatol. 41 (3) (2004) 436–445, https://doi.org/10.1016/J.JHEP.2004.05.018.
[43] J. Zhang, Y. Liu, G. Shi, Gene microarray analysis of expression profiles in suberoyllanilide hyroxamic acid-treated dendritic cells, Biochem. Biophys. Res. Commun. 508 (2) (2019) 392–397, https://doi.org/10.1016/J.BBRC.2018.11.143.
[44] J. Meng, H.H. Zhang, C.X. Zhou, C. Li, F. Zhang, Q.B. Mei, The histone deacetylase inhibitor trichostatin a induces cell cycle arrest and apoptosis in colorectal cancer cells via p53-dependent and -independent pathways, Oncol. Rep. 28 (1) (2012) 384–388, https://doi.org/10.3892/OR.2012.1793.
[45] K. Bajbouj, C. Mawrin, R. Hartig, J. Schulze-Luehrmann, A. Wilisch-Neumann, A. Roessner, et al., P53-dependent antiproliferative and pro-apoptotic effects of trichostatin a (TSA) in glioblastoma cells, J. Neurooncol. 107 (3) (2012) 503–516, https://doi.org/10.1007/S11060-011-0791-2.
[46] C.Z.Y. Zhang, G.G. Chen, J.L. Merchant, P.B.S. Lai, Interaction between ZBP-89 and p53 mutants and its contribution to effects of HDACi on hepatocellular carcinoma, Cell Cycle 11 (2) (2012) 322–334, https://doi.org/10.4161/CC.11.2.18758.
[47] T.E. Fandy, S. Shankar, D.D. Ross, E. Sausville, R.K. Srivastava, Interactive effects of HDAC inhibitors and TRAIL on apoptosis are associated with changes in mitochondrial functions and expressions of cell cycle regulatory genes in multiple myeloma, Neoplasia 7 (7) (2005) 646–657, https://doi.org/10.1593/NEO.04655.
[48] Y. Zu, Z. Yang, S. Tang, Y. Han, J. Ma, Effects of P-Glycoprotein and its inhibitors on apoptosis in K562 cells, Molecules 19 (9) (2014) 13061–13075, https://doi.org/10.3390/MOLECULES190913061.
[49] Á. Jóna, N. Khaskhely, D. Buglio, J.A. Shafer, E. Derenzini, C.M. Bollard, et al., The histone deacetylase inhibitor entinostat (SNDX-275) induces apoptosis in hodgkin lymphoma cells and synergizes with Bcl-2 family inhibitors, Exp. Hematol. 39 (10) (2011) 1007–1017, https://doi.org/10.1016/J.EXPHEM.2011.07.002.
[50] A. Pandya Martin, M.A. Park, C. Mitchell, T. Walker, M. Rahmani, A. Thorburn, et al., BCL-2 family inhibitors enhance histone deacetylase inhibitor and sorafenib lethality via autophagy and overcome blockade of the extrinsic pathway to facilitate killing, Mol. Pharm. 76 (2) (2009) 327–341, https://doi.org/10.1124/mol.109.056309.
[51] T.T.T. Nguyen, Y. Zhang, E. Shang, C. Shu, C.M. Quinzii, M.A. Westhoff, et al., Inhibition of HDAC1/2 along with TRAP1 causes synthetic lethality in glioblastoma model systems, Cells 9 (7) (2020) 1661, https://doi.org/10.3390/CELLS9071661.
[52] Y.J. Wang, Q. Li, H. Xiao, Bin, Y.J. Li, Q. Yang, X.X. Kan, et al., Chamaejasmin b exerts anti-MDR effect in vitro and in vivo via initiating mitochondria-dependant

intrinsic apoptosis pathway, Drug Des. Devel Ther. 9 (2015) 5301–5313, https://doi.org/10.2147/DDDT.S89392.
[53] P. Vasefifar, S. Najafi, R. Motafakkerazad, M. Amini, S. Safaei, B. Najafzadeh, et al., Targeting nanog expression increased cisplatin chemosensitivity and inhibited cell migration in gastric cancer cells, Exp. Cell Res. 429 (2) (2023) 113681, https://doi.org/10.1016/J.YEXCR.2023.113681.
[54] M. Sanaei, F. Kavoosi, Effects of trichostatin a on the intrinsic and extrinsic apoptotic pathway, cell viability, and apoptosis induction in hepatocellular carcinoma cell lines, Gastroenterol. Hepatol. Bed. Bench 14 (4) (2021) 323–333.
[55] P.S. Moore, S. Barbi, M. Donadelli, C. Costanzo, C. Bassi, M. Palmieri, et al., Gene expression profiling after treatment with the histone deacetylase inhibitor trichostatin a reveals altered expression of both pro- and anti-apoptotic genes in pancreatic adenocarcinoma cells, Biochim. Biophys. Acta 1693 (3) (2004) 167–176, https://doi.org/10.1016/J.BBAMCR.2004.07.001.
[56] J.K. Kim, J. Guan, I. Chang, X. Chen, D. Han, C.Y. Wang, PS-341 and histone deacetylase inhibitor synergistically induce apoptosis in head and neck squamous cell carcinoma cells, Mol. Cancer Ther. 9 (7) (2010) 1977–1984, https://doi.org/10.1158/1535-7163.MCT-10-0141.
[57] C. Henderson, M. Mizzau, G. Paroni, R. Maestro, C. Schneider, C. Brancolini, Role of caspases, bid, and p53 in the apoptotic response triggered by histone deacetylase inhibitors Trichostatin-A (TSA) and suberoylanilide hydroxamic acid (SAHA), J. Biol. Chem. 278 (14) (2003) 12579–12589, https://doi.org/10.1074/JBC.M213093200.
[58] S. Götze, M. Coersmeyer, O. Müller, S. Sievers, Histone deacetylase inhibitors induce attenuation of wnt signaling and TCF7L2 depletion in colorectal carcinoma cells, Int. J. Oncol. 45 (4) (2014) 1715–1723, https://doi.org/10.3892/IJO.2014.2550.
[59] J. Domingo-Domènech, R. Pippa, M. Tápia, P. Gascón, O. Bachs, M. Bosch, Inactivation of NF-kappaB by proteasome inhibition contributes to increased apoptosis induced by histone deacetylase inhibitors in human breast cancer cells, Breast Cancer Res. Treat. 112 (1) (2008) 53–62, https://doi.org/10.1007/S10549-007-9837-8.
[60] Y. Fang, Y. Hu, P. Wu, B. Wang, Y. Tian, X. Xia, et al., Synergistic efficacy in human ovarian cancer cells by histone deacetylase inhibitor TSA and proteasome inhibitor PS-341, Cancer Invest. 29 (4) (2011) 247–252, https://doi.org/10.3109/07357907.2010.496756.
[61] A.P. Morales, A.C.P. Carvalho, P.T. Monteforte, H. Hirata, S.W. Han, Y.T. Hsu, et al., Endoplasmic reticulum calcium release engages bax translocation in cortical astrocytes, Neurochem. Res. 36 (5) (2011) 829–838, https://doi.org/10.1007/S11064-011-0411-8.
[62] L. Zhang, L. Li, H. Liu, J.L. Borowitz, G.E. Isom, BNIP3 mediates cell death by different pathways following localization to endoplasmic reticulum and mitochondrion, FASEB J. 23 (10) (2009) 3405–3414, https://doi.org/10.1096/FJ.08-124354.
[63] R.G. Jones, T. Bui, C. White, M. Madesh, C.M. Krawczyk, T. Lindsten, et al., The proapoptotic factors bax and bak regulate t cell proliferation through control of endoplasmic reticulum Ca(2+) homeostasis, Immunity 27 (2) (2007) 268–280, https://doi.org/10.1016/J.IMMUNI.2007.05.023.
[64] R.F. Place, E.J. Noonan, C. Giardina, HDAC inhibition prevents NF-κB activation by suppressing proteasome activity: Down-regulation of proteasome subunit expression stabilizes IκBα, Biochem. Pharm. 70 (3) (2005) 394–406, https://doi.org/10.1016/J.BCP.2005.04.030.
[65] L. Gaiaschi, C. Casali, A. Stabile, S. D'Amico, M. Ravera, E. Gabano, et al., DNA damage repair in glioblastoma: a novel approach to combat drug resistance, Cell Prolif. 58 (6) (2025) e13815, https://doi.org/10.1111/CPR.13815.
[66] D.G. Breckenridge, M. Germain, J.P. Mathai, M. Nguyen, G.C. Shore, Regulation of apoptosis by endoplasmic reticulum pathways, Oncogene 22 (53) (2003) 8608–8618, https://doi.org/10.1038/sj.onc.1207108.
[67] S. Jang, H.S. Jeong, Histone deacetylase inhibition-mediated neuronal differentiation via the wnt signaling pathway in human adipose tissue-derived mesenchymal stem cells, Neurosci. Lett. 668 (2018) 24–30, https://doi.org/10.1016/J.NEULET.2018.01.006.
[68] J.M. Shieh, Y.A. Tang, F.H. Hu, W.J. Huang, Y.J. Wang, J. Jen, et al., A histone deacetylase inhibitor enhances expression of genes inhibiting wnt pathway and augments activity of DNA demethylation reagent against nonsmall-cell lung cancer, Int. J. Cancer 140 (10) (2017) 2375–2386, https://doi.org/10.1002/IJC.30664.
[69] S.J. Kim, S. Kim, Y.J. Choi, U.J. Kim, K.W. Kang, CKD-581 downregulates Wnt/β-Catenin pathway by DACT3 induction in hematologic malignancy, Biomol. Ther. (Seoul) 30 (5) (2022) 435–446, https://doi.org/10.4062/BIOMOLTHER.2022.022.
[70] M.R. Makena, M. Ko, D.K. Dang, R. Rao, Epigenetic modulation of SPCA2 reverses epithelial to mesenchymal transition in breast cancer cells, Cancers (Basel) 13 (2) (2021) 359, https://doi.org/10.3390/cancers13020259.
[71] A. Shamsian, M.R. Sepand, M.J. Kachousangi, T. Dara, S.N. Ostad, F. Atyabi, et al., Targeting tumorigenicity of breast cancer stem cells using SAHA/Wnt-b catenin antagonist loaded onto protein corona of gold nanoparticles, Int. J. Nanomed. 15 (2020) 4063–4078, https://doi.org/10.2147/IJN.S234636.
[72] W. Yang, Y. Li, R. Gao, Z. Xiu, T. Sun, MHC class I dysfunction of glioma stem cells escapes from CTL-mediated immune response via activation of Wnt/β-catenin signaling pathway, Oncogene 39 (5) (2020) 1098–1111, https://doi.org/10.1038/s41388-019-1045-6.
[73] Y. Wang, M. Liu, Y. Jin, S. Jiang, J. Pan, In vitro and in vivo anti-uveal melanoma activity of JSL-1, a novel HDAC inhibitor, Cancer Lett. 400 (2017) 47–60, https://doi.org/10.1016/J.CANLET.2017.04.028.
[74] Z. Yang, W. Su, Q. Zhang, L. Niu, B. Feng, Y. Zhang, et al., Lactylation of HDAC1 confers resistance to ferroptosis in colorectal cancer, Adv. Sci. (Weinh) 12 (12) (2025) e2408845, https://doi.org/10.1002/ADVS.202408845.
[75] M. Zille, A. Kumar, N. Kundu, M.W. Bourassa, V.S.C. Wong, D. Willis, et al., Ferroptosis in neurons and cancer cells is similar but differentially regulated by histone deacetylase inhibitors, ENEURO.0263-18.2019, eNeuro 6 (1) (2019), https://doi.org/10.1523/ENEURO.0263-18.2019.
[76] L. Shao, S. Yu, W. Ji, H. Li, Y. Gao, The contribution of necroptosis in neurodegenerative diseases, Neurochem. Res. 42 (8) (2017) 2117–2126, https://doi.org/10.1007/S11064-017-2249-1.
[77] L. Yuan, Z. Wang, L. Liu, X. Jian, Inhibiting histone deacetylase 6 partly protects cultured rat cortical neurons from oxygen-glucose deprivation-induced necroptosis, Mol. Med. Rep. 12 (2) (2015) 2661–2667, https://doi.org/10.3892/MMR.2015.3779.
[78] D. Bollino, I. Balan, L. Aurelian, Valproic acid induces neuronal cell death through a novel calpain-dependent necroptosis pathway, J. Neurochem. 133 (2) (2015) 174–186, https://doi.org/10.1111/JNC.13029.
[79] D. Karagiannis, W. Wu, A. Li, M. Hayashi, X. Chen, M. Yip, et al., Metabolic reprogramming by histone deacetylase inhibition preferentially targets NRF2-activated tumors, Cell Rep. 43 (1) (2024) 113629, https://doi.org/10.1016/j.celrep.2023.113629.
[80] R. Teena, U. Dhamodharan, D. Ali, K. Rajesh, K.M. Ramkumar, Gene expression profiling of multiple histone deacetylases (HDAC) and its correlation with NRF2-mediated redox regulation in the pathogenesis of diabetic foot ulcers, Biomolecules 10 (10) (2020) 1466, https://doi.org/10.3390/BIOM10101466.
[81] R. Bian, Y. Shang, N. Xu, B. Liu, Y. Ma, H. Li, et al., HDAC inhibitor enhances ferroptosis susceptibility of AML cells by stimulating iron metabolism, Cell Signal 127 (2025) 111583, https://doi.org/10.1016/j.cellsig.2024.111583.
[82] L. Zhu, T. Zhou, L. Wu, X. Zhu, L. Chen, M. Zhang, et al., Microglial exosome TREM2 ameliorates ferroptosis and neuroinflammation in alzheimer's disease by activating the Wnt/β-catenin signaling, Sci. Rep. 15 (1) (2025) 24968, https://doi.org/10.1038/S41598-025-09563-1.
[83] B. Xue, L. Yan, M. Ye, D. Gu, J. Qian, N. He, et al., PROTAC-Surufatinib suppresses pancreatic neuroendocrine neoplasms progression by inducing ferroptosis through inhibiting WNT/β-catenin pathway mediated by HMOX1, Int. J. Biol. Sci. 21 (6) (2025) 2476–2492, https://doi.org/10.7150/IJBS.106357.
[84] S. Gao, X. Wang, Z. Shao, J. Chen, MGST1 inhibits Sevoflurane-Induced ferroptosis and activates the wnt pathway in HT22 cells, Mol. Neurobiol. 62 (7) (2025) 9497–9505, https://doi.org/10.1007/S12035-025-04841-5.